



FATİH UNIVERSITY

The Graduate School of Sciences and Engineering

**Master of Science in
Physics**

SAMPLE SPINE

**A DFT STUDY ON ELECTRONIC PROPERTIES OF
TRANSITION METAL DOPED BORON NITRIDE
NANOTUBES**

by

Yunus KAYA

January 2015



**A DFT STUDY ON ELECTRONIC PROPERTIES OF TRANSITION
METAL DOPED BORON NITRIDE NANOTUBES**

by

Yunus KAYA

A thesis submitted to

the Graduate School of Sciences and Engineering

of

Fatih University

in partial fulfillment of the requirements for the degree of

Master of Science

in

Physics

January 2015
Istanbul, Turkey

APPROVAL PAGE

This is to certify that I have read this thesis written by Yunus KAYA and that in my opinion it is fully adequate, in scope and quality, as a thesis for the degree of Master of Science in Physics.

Prof. Serkan ÇALIŞKAN
Thesis Supervisor

I certify that this thesis satisfies all the requirements as a thesis for the degree of Master of Science in Physics.

Prof. Mustafa KUMRU
Head of Department

Examining Committee Members

Prof. Serkan ÇALIŞKAN

Prof. Sadık GÜNER

Assoc. Prof. Levent SARI

It is approved that this thesis has been written in compliance with the formatting rules laid down by the Graduate School of Sciences and Engineering.

Prof. Nurullah ARSLAN
Director

January 2015

A DFT STUDY ON ELECTRONIC PROPERTIES OF TRANSITION METAL DOPED BORON NITRIDE NANOTUBES

Yunus KAYA

M.S. Thesis – Physics
January 2015

Thesis Supervisor: Prof. Dr. Serkan ÇALIŞKAN

ABSTRACT

In this thesis, we mainly concentrated on spin unrestricted electronic structure properties of boron nitride nanotubes (BNNTs). In order to reveal these properties, Density Functional Theory (DFT) calculations were performed through the software package Atomistix ToolKit (ATK). Both pure and doped BNNTs with infinite lengths were examined, modifying the tube radius. Substitutionally doped transition metal atoms were employed to observe the possible spin dependent behavior and/or to expose the magnetism in BNNTs. Hence, we also investigated the magnetic properties of doped BNNTs with low concentration of dopants. In general, we considered *zigzag* BNNTs with chiral vectors $(n,m) = (4,0)$, $(6,0)$ and $(8,0)$. The DFT calculations showed that the energy band gap of a BNNT and the electronic structure behavior were determined by its chiral vector or radius. The density of states spectra of pure BNNTs were spin symmetric, however, those of doped ones are spin asymmetric, yielding spin polarization or spin dependent electronic structure properties. Moreover, it was obtained that both the position and type of dopants govern spin resolved electronic transport. BNNTs can be utilized in novel technology and applied in the field of spintronics as fundamental structures.

Keywords: Boron Nitride Nanotubes, Transition Metals, Density Functional Theory, *first-principles* calculations, Electronic Structure.

GEÇİŞ METAL KATKILI BOR NİTRÜR NANOTÜPLERİN ELEKTRONİK ÖZELLİKLERİ ÜZERİNE DFT ÇALIŞMASI

Yunus KAYA

Yüksek Lisans Tezi – Fizik
Ocak 2015

Tez Danışmanı: Prof. Dr. Serkan ÇALIŞKAN

ÖZ

Bu tezde başlıca bor nitrür nanotüplerin (BNNTler) spine bağlı elektronik yapı özelliklerine odaklanılmıştır. Bu özellikleri inceleyebilmek için Atomistix Toolkit (ATK) adlı bir yazılım paketi vasıtasıyla Yoğunluk Fonksiyonel Teorisi (DFT) hesaplamaları yapılmıştır. Tüp yarıçapları değiştirilerek oluşturulan sonsuz uzunlukta saf ve katkılı BNNTler incelenmiştir. BNNTlerde ortaya çıkabilecek manyetizma ve/veya muhtemel spine bağlı davranışı gözlemek için, sistemdeki atomların yerine geçen geçiş metal atomlarından oluşan katkılar kullanılmıştır. Bu nedenle, katkı konsantrasyonu düşük katkılı BNNTlerin manyetik özellikleri de incelenmiştir. Genel olarak, kiral vektörleri $(n,m) = (4,0)$, $(6,0)$ ve $(8,0)$ olan *zigzag* BNNTler incelenmiştir. DFT hesaplamalarının sonuçlarına göre, bir BNNTnin enerji bant boşluğu ve elektronik yapı davranışı kiral vektörü ve yarıçapı tarafından belirlenmiştir. Saf BNNTlerin durum yoğunluğu spektrumları spin simetrik olmasına rağmen, geçiş metal atom katkılı olanların spektrumları spin asimetrik elde edilmiştir. Bu durum, spin polarizasyonuna veya spine bağlı elektronik yapı özelliklerine sebep olmaktadır. Ayrıca, hem katkı türünün hem de katkı konumunun spine bağlı elektronik transportu yönlendirdiği gözlemlenmiştir. BNNTler spintronik alanında ve yeni teknolojide temel yapılar olarak kullanılabilir yapılarıdır.

Anahtar Kelimeler: Bor Nitrür Nanotüpler, Geçiş Metalleri, Yoğunluk Fonksiyonel Teorisi, *temel ilkeler* hesaplamaları, Elektronik Yapı.

To my mother, father , wife
and children...

ACKNOWLEDGEMENT

I would like to express my sincere gratitude to my advisor Prof. Dr. Serkan ÇALIŞKAN for the continuous support of my M.S. Thesis study and research.

I express my thanks and appreciation to my family for their understanding, motivation and patience.

TABLE OF CONTENTS

ABSTRACT.....	iii
ÖZ	iv
DEDICATION.....	v
ACKNOWLEDGMENT	vi
TABLE OF CONTENTS.....	vii
LIST OF TABLES	ix
LIST OF FIGURES	x
LIST OF SYMBOLS AND ABBREVIATIONS	xii
CHAPTER 1 INTRODUCTION	1
CHAPTER 2 LITERATURE REVIEW	3
2.1 Nanotechnology.....	3
2.1.1 Importance of Nanotechnology.....	4
2.1.2 Benefits of Nanotechnology.....	4
2.1.3 Disadvantage of Nanotechnology	5
2.2 Nanotubes.....	6
2.2.1 Carbon Nanotubes (CNTs).....	7
2.2.1.1 Properties of CNTs.....	8
2.2.1.2 Applications of CNTs.....	9
2.3 Boron Nitride.....	9
2.3.1 Characteristics of Boron.....	9
2.3.2 Boron Nitride (BN)	10
2.3.3 Hexagonal Boron Nitride (h-BN).....	10
2.4 Boron Nitride Nanotubes (BNNTs).....	11
2.4.1 Application Areas of BNNTs.....	13
2.4.2 Synthesis Methods of BNNTs.....	13
2.4.3 Properties of BNNTs.....	14
2.4.3.1 Mechanical Properties of BNNTs	15

2.4.3.2	Electrical Properties of BNNTs.....	15
2.4.3.3	Thermal Conductivity of BNNTs.....	16
2.4.3.4	Thermal Oxidation Resistance of BNNTs.....	16
2.4.3.5	Optical properties of BNNTs	16
2.5	Spintronics	17
CHAPTER 3	THE METHOD.....	19
3.1	Atomistix Toolkit (ATK).....	19
3.2	Density Functional Theory (DFT).....	20
3.3	Green's Function (GF) Formalism.....	23
3.4	Non Equilibrium Green's Function Formalism (NEGF).....	24
CHAPTER 4	CALCULATIONS AND RESULTS.....	26
4.1	Systems and DFT Parameters.....	26
4.2	Pure BNNTs	27
4.2.1	System BN-4	27
4.2.2	System BN-6	29
4.2.3	System BN-8	32
4.3	Doped BNNTs.....	34
4.3.1	Co Doped BN-4.....	36
4.3.2	Cr Doped BN-4	38
4.3.3	Ni Doped BN-4	39
4.3.4	Au Doped BN-4	41
4.4	Position of Transition Metal Atom.....	45
CHAPTER 5	CONCLUSION.....	47
REFERENCES	49

LIST OF TABLES

TABLE

2.1	Comparison of BNNTs and CNTs.	14
4.1	Band gap values for zigzag BN-4, BN-6 and BN-8.....	34
4.2	Comparison of band gaps of zigzag pure BN-4, Co doped BN-4, Cr doped BN-4, Ni doped BN-4 and Au doped BN-4.	44
4.3	Average magnetic moment per atom, emerging in Co doped BN-4, Cr doped BN-4, Ni doped BN-4 and Au doped BN-4, for a specific dopant concentration.....	44
4.4	Spin dependent band gap of a zigzag Co doped BN-4 when Co atom is placed in the middle, at the left and right side of the BN-4.	46

LIST OF FIGURES

FIGURE

2.1	Comparison of sizes of the world, ball and fullerene.....	3
2.2	Connection of science and nanotechnology	5
2.3	Different types of nanotubes	6
2.4	Schematic diagrams showing the different form of carbon structures.....	7
2.5	Graphene structures with certain directions: Zigzag, armchair and helical	8
2.6	(a) BN particles, size 1-2 μm , (b) BN particles, size 7-10 μm	10
2.7	Hexagonal form of BN	11
2.8	The number of publications on (a) CNTs, and (b) BNNTs.....	12
2.9	Representative TEM image of BNNTs grown at NASA Langley Research Center (LaRC)	14
3.1	Geometry of a device system consisting of a central region and two electrodes..	25
4.1	Base and side views of zigzag BN-4 in the unit cell where the axis in yellow denotes the z (tube) axis. B and N atoms are shown in rose and blue, respectively	28
4.2	DOS spectrum for zigzag BN-4 in the absence of spin.....	29
4.3	Base view of zigzag BN-6 in the unit cell. B and N atoms are shown in rose and blue, respectively.	30
4.4	DOS spectrum for zigzag BN-6 in the absence of spin.....	31
4.5	DOS spectrum for zigzag BN-6 in the presence of spin	31
4.6	Base view of zigzag BN-8 in the unit cell. B and N atoms are shown in rose and blue, respectively	32
4.7	DOS for a zigzag BN-8 in the absence of spin.....	32
4.8	DOS for a zigzag BN-8 in the presence of spin	33
4.9	Side views of (a) BN-4, (b) BN-6 and (c) BN-8, repeated 3 times along z axis...	35

4.10	Side and base views of zigzag Co doped BN-4 in the supercell where the axis in yellow denotes the z (tube) axis. B, N and Co atoms are shown in rose, blue and dark pink, respectively	36
4.11	DOS spectrum of zigzag Co doped BN-4 in the presence of spin. Black (positive) and red (negative) variations indicate the majority and minority DOS, respectively.	37
4.12	Side and base views of zigzag Cr doped BN-4 in the supercell where the axis in yellow denotes the z (tube) axis. B, N and Cr atoms are shown in rose, blue and purple, respectively	38
4.13	DOS spectrum of zigzag Cr doped BN-4 in the presence of spin. Black (positive) and red (negative) variations indicate the majority and minority DOS, respectively.....	39
4.14	Side view of zigzag Ni doped BN-4 in the supercell where the axis in yellow denotes the z (tube) axis. B, N and Ni atoms are shown in rose, blue and green, respectively..	40
4.15	DOS spectrum of zigzag Ni doped BN-4 in the presence of spin. Black (positive) and red (negative) variations indicate the majority and minority DOS, respectively..	41
4.16	Side view of zigzag Au doped BN-4 in the supercell where the axis in yellow denotes the z (tube) axis. B, N and Au atoms are shown in rose, blue and yellow, respectively.	42
4.17	DOS spectrum of zigzag Au doped BN-4 in the presence of spin. Black (positive) and red (negative) variations indicate the majority and minority DOS, respectively.	42
4.18	Zigzag Co doped system. Co is located at (a) left and (b) right side of BN-4 in the supercell. B, N and Co atoms are shown in rose, blue and dark pink, respectively..	45

LIST OF SYMBOLS AND ABBREVIATIONS

SYMBOL/ABBREVIATION

Å	Angstrom
ATK	Atomistix Toolkit
Au	Gold
BN	Boron Nitride
BNNTs	Boron Nitride Nanotubes
cBN	Cubic Boron Nitride
CNTs	Carbon Nanotubes
Co	Cobalt
Cr	Chromium
CVD	Chemical Vapor Deposition
DFT	Density Functional Theory
DOS	Density of States
DWCNT	Double Walled Carbon Nanotube
$E(n)$	Energy Functional
$E_{xc}(n)$	Exchange Correlation Energy Functional
E_F	Fermi Energy
E_g	Energy Gap
eV	Electron Volt
GF	Green's Function
GGA	Generalized Gradient Approximation
h-BN	Hexagonal Boron Nitride
LDA	Local Density Approximation
MWCNT	Multi Walled Carbon Nanotube
NEGF	Non Equilibrium Green's Function
Ni	Nickel
PBE	Perdew-Burke-Ernzerhof

PZ	Perdew-Zunger
SWCNT	Single Walled Carbon Nanotube
TEM	Transmission Electron Microscopy
U	Hubbard Term
UV	Ultraviolet
$V_{\text{ext}}(\mathbf{r})$	External Potential
XC	Exchange Correlation
$n(\mathbf{r})$	Ground State Electron Density
μ_B	Bohr Magnetron
Σ_L	Self Energy of the Left Electrode
Σ_R	Self Energy of the Right Electrode
Ψ	Wave Function
$\Psi(\mathbf{r}_1, \mathbf{r}_2, \dots, \mathbf{r}_N)$	Many-Body Wave Function

CHAPTER 1

INTRODUCTION

Nanotechnology is a field which considers the substances of sizes ranging from 1 nm to 100 nm (Sellers K., 2010). Nanotechnology has many potential benefits including energy savings, improving renewable energy sources, production process, environmental protection, agriculture applications and medical innovation. The investigation of nanoscale structures is going on and their applications on technology are still not known exactly.

Nanotube is an important branch of nanotechnology. Nanotubes are cylindrical structures made through rolling of two dimensional sheets. They are formed in hollow fibers with a wall whose thickness is only one atom wide. They are strong and display many thermal and electrical properties so that they can be used in nanotechnology, for instance, as resistors, capacitors, inductors, diodes and transistors.

Among the nanotubes, carbon nanotubes (CNTs) are common ones. CNTs were first studied by Japanese researchers in the early 1990s (Iijima S., 1991). There are wide range of applications due to two important properties of CNTs: Unusual strength and unique electrical properties (Purohit R. et al., 2014). Boron nitride nanotubes (BNNTs) have the same atomic structure as CNTs, however, the properties of them are very different from CNTs. A BNNT is an electrical insulator with a wide band gap, but CNTs can be metallic or semiconducting. Moreover, BNNTs are more resistant to oxidation compared to CNTs (Wang J. et al., 2010).

The purpose of this thesis is to investigate, in general, spin unrestricted electronic structure properties of both pure and transition metal doped zigzag BNNTs. In general, we focused on bulk BNNT structures defined in supercells. The transport and magnetic properties were examined in terms of tube radius and type of transition metal atom. The

tube radius is determined by its chiral vector (n,m) . For the zigzag BNNTs with chiral vectors $(n,m) = (4,0)$, $(6,0)$ and $(8,0)$, first principles density functional theory (DFT) calculations were performed, applying the software package called Atomistix Toolkit (ATK). The ATK is based on DFT through which one can analyze both electronic and magnetic properties of nanoscale systems in the presence of spin. Thus ATK can simulate the spin unrestricted behavior of nanostructures.

In this thesis, we intended to make a detailed analysis of both pure and transition metal doped BNNTs. We worked as follows;

- We constructed pure zigzag BNNTs with a few radii and doped them with various transition metals. Infinite bulk BNNT structures were constructed in the supercells with appropriate lattice parameters. Then they were optimized (atomic-scale relaxation) to mimic stable structures.
- We investigated these structures to expose the spin unrestricted electronic structure, transport and magnetic properties. We have obtained the relevant quantities and plotted band structure and density of states. We have tried to examine the effect of dopant type and other factors on these structures.

This thesis is divided into 5 parts: In Chapter 2, we give a literature review nanotubes (both CNTs and BNNTs); In Chapter 3, the computational method employed in software package ATK is introduced; In Chapter 4, for a few zigzag pure and doped BNNTs, the calculation results and discussions are presented; In Chapter 5, conclusion is given.

CHAPTER 2

LITERATURE REVIEW

2.1 NANOTECHNOLOGY

Before the description of nanotechnology, it is better to define the term “nano”. The meaning of nano is one billionth. The nanometer scale of a meter is about one billionth or about ten thousandth of the thickness of a human hair. Nanotechnology which considers the substances in nanoscales, from 1 nm up to 100 nm, is an important area of science (Hussein A.K., 2014). Nanotechnology includes the production of novel structures and the formation of new substances by changing molecular structure of known materials.

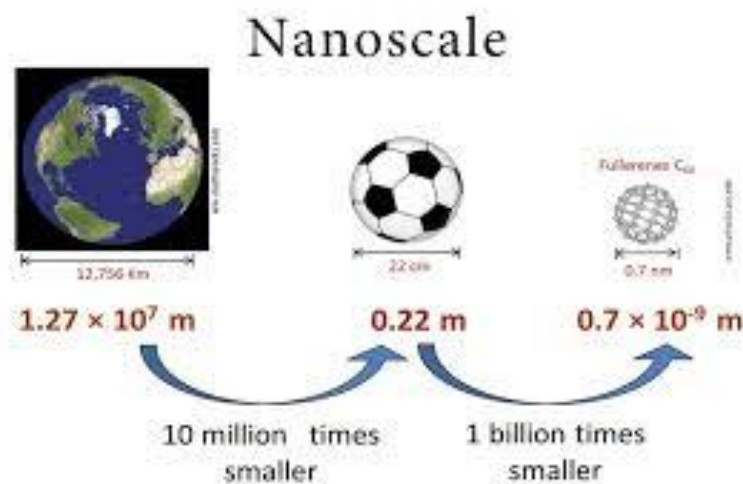


Figure 2.1 Comparison of sizes of the world, ball and fullerene (www.kilo-pico.com)

If the atomic sequence in nature can be copied or moved, many various formations of substances can be achieved. Nowadays, this idea increases the interest in nanotechnology and accelerates the associated studies in this area. Many existing limits in the science can be overcome and the form of a substance can be changed, such as formation of coal into diamond.

2.1.1 Importance of Nanotechnology

During the production of materials through nanotechnology, one may achieve sufficiently high energy. As a consequence of this, functional superb products can be obtained. Nanotechnology has the capacity to revolutionize health technology, textile, paint, chemicals, stone, water treatment, electronics, healthcare, automotive, computer technology and all branches of industry (Porter A.L. and Youtie J, 2009). In recent years approximately \$1.6 trillion is spent for nanotechnology worldwide in a year (Mohammad A.W. et al., 2011).

Nanotechnology is known as a novel branch of science and engineering. However some researchers fear that there may be disadvantages to humans and the environment that we don't know yet, for instance, tiny nanoparticles may be toxic under certain circumstances.

2.1.2 Benefits of Nanotechnology

There are many benefits of nanotechnology as described below;

- Nanotechnology means saving.
- Cost of energy can be reduced by using nanotechnology.
- Improved renewable energy sources using nanotechnology can be alternative.
- Nanomaterials can be used as cleaners in the textile, the surface of the material etc.
- Via nanotechnology, materials may have more efficient usage and high quality. For instance, plastics or metals with CNTs lead low consumption of fuel, as airplanes and vehicles made of CNTs become lighter (Hussein A.K., 2014).
- Nanotechnology plays an important role in national income levels.

- Nanotechnology enables improvement of quality of life.
- One can upgrade the quality of a product.
- Production with nanotechnology can offer improves the quality of people's living standards, healthier and more secure life.
- Countries using nanotechnology go forward without having to restore the international technology race (Dowling A.P., 2004).

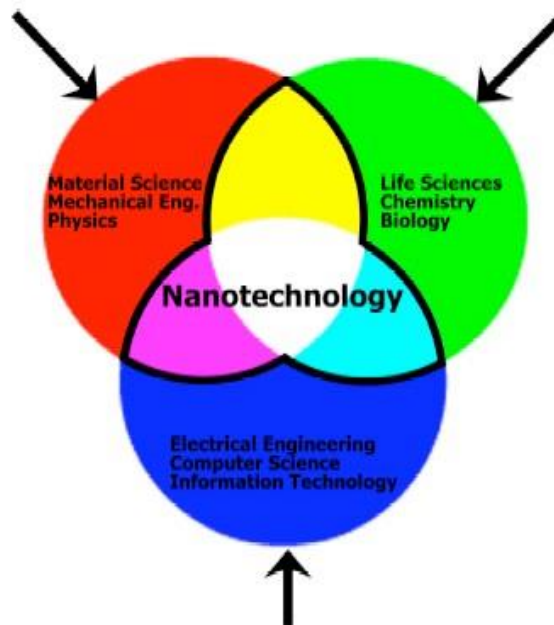


Figure 2.2 Connection of science and nanotechnology (www.nanomed.yolasite.com)

2.1.3 Disadvantage of Nanotechnology

There are also some disadvantages of nanotechnology. They are given as follows;

- Ultra-small particles used in the diesel engines, powerplants and fiery machinery can cause great damage in the lungs of humans. Metals and hydrocarbons are hosting inside.
- Nanoparticles, since they are nanoscale particles, are able to move into the body through the skin and can easily reach, for instance, lungs and digestive system. This may cause reproduction of cell-damaging particles.
- Nanoparticles are left in nature for absorbing.

- Cloning, highly qualified soldiers and robots can be constructed. It leads to disproportion at power in technology (Ekli E. and Şahin N., 2010).

2.2 NANOTUBES

Nanotube is an important branch of nanotechnology. Nanotubes are cylindrical structures made through rolling of two dimensional sheets. They are formed in hollow fibers with a wall whose thickness is only one atom wide. Nanotubes appear as dust or black soot. They are strong and display many thermal and electrical properties so that they can be used in nanotechnology, for instance, as resistors, capacitors, inductors, diodes and transistors. Among the nanotubes, CNTs are the common ones. CNTs were first studied by Japanese researchers in the early 1990s (Iijima S., 1991).

Nanotubes which can be constructed in a laboratory are strong and display interesting thermal and electrical properties so that they are able to be used in nanotechnology as, for instance, resistors, capacitors, inductors, diodes and transistors. Nanotubes can be classified by the number of homocentric cylinders, radius and length of cylinder. Nanotubes can be grown in terms of *chirality* defined by chiral vector (n,m) . Multiple nanotubes can be installed into microscopic mechanical systems, known as nanomachines.

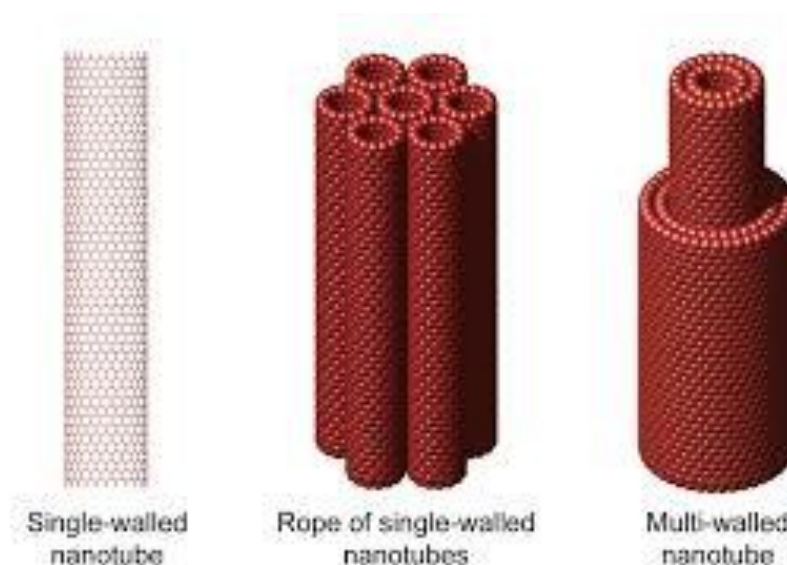


Figure 2.3 Different types of nanotubes (www.nanotechnologies.qc.ca)

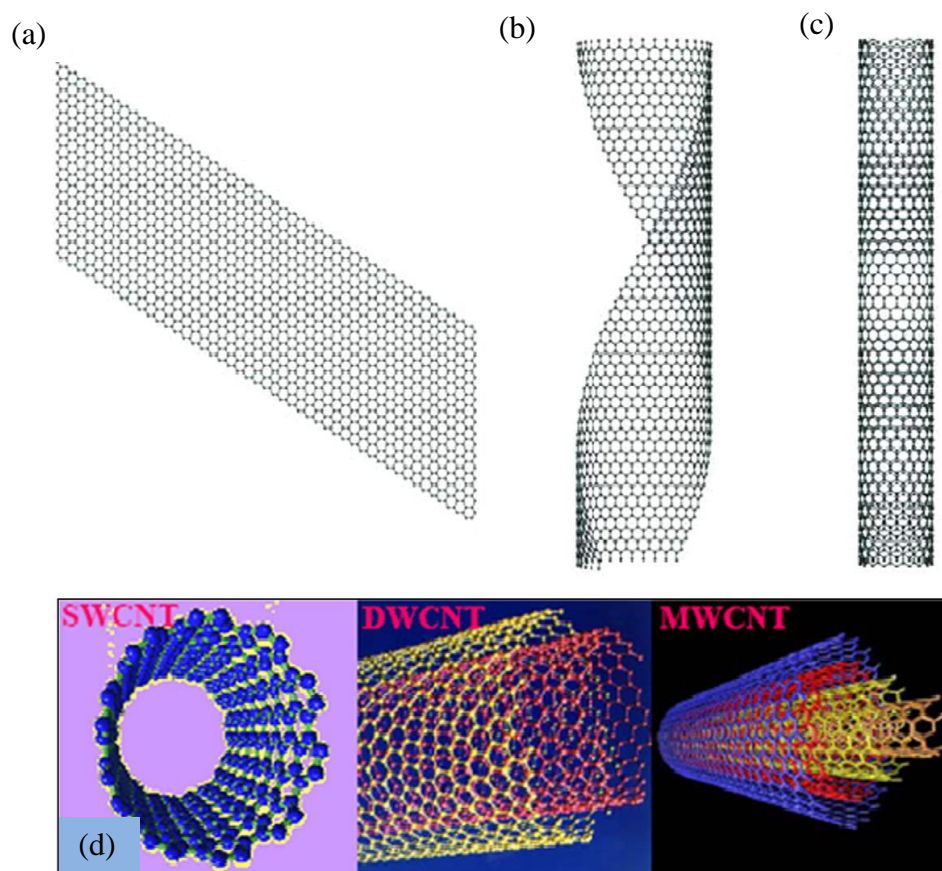


Figure 2.4 Schematic diagrams showing the different form of carbon structures: (a) Flat sheet of graphite (graphene), (b) Partially rolled sheet of graphite, (c) Single wall CNT (SWCNT), (d) Structures of three forms of CNTs: SWCNT, double-walled CNT (DWCNT) and multi-walled CNT (MWCNT), respectively (Aqel A. et al.,2012).

2.2.1 Carbon Nanotubes (CNTs)

CNTs are thin and hollow cylindrical structures showing enormous electrical and optical characteristics. CNTs having interesting and unusual properties are used in electronics, optics, materials science and other fields of technology. Two most striking features are especially important for such a wide range of applications; Unusual strength and unique electrical properties (Purohit R. et al., 2014). Two main types of a CNT are the single and multi-walled nanotubes (see Figure 2.4d). Besides there are also some other rare types such as nanobuds and nanotorus.

Graphene is a sheet structure, which can be formed in *zigzag* and *armchair* orientations or through a *chirality* as shown in Figure 2.5. These forms are defined by chiral vector (n,m) . $(n,0)$, (n,n) and (n,m) give the zigzag, armchair and helical tubes,

respectively. Rolling of a sheet structure along the directions given in Figure 2.5 yields the associated CNTs.

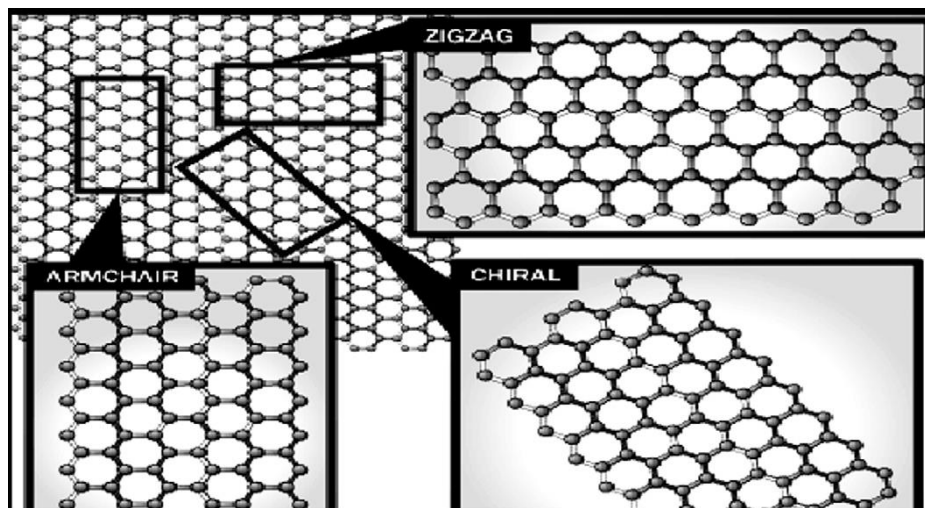


Figure 2.5 Graphene structures with certain directions: Zigzag, armchair and helical (Aqel A. et al.,2012).

2.2.1.1 Properties of CNTs

Molecular electronic and structural characteristics of a CNT are largely determined by its stable one-dimensional structure. Distinct physical and chemical properties of nanotubes can be achieved by modifying the geometrical structure of them. The most important properties of CNTs are related to

- chemical reactivity
- electrical conductivity
- optical activity
- mechanical strength

The elastic modulus of CNTs is 1Tpa and 100 times more resistant than steel with the same weight. The elastic modulus of the diamond is 1.2 Tpa, which is close that of CNTs. Hence, CNTs are sufficiently durable (Guptaa A.K. and Harshaa S.P, 2014). Another important feature of CNTs is that their electrical current density is thousand times more than copper (Purohit R. et al., 2014). Furthermore various properties of CNTs indicated that they can protect themselves better than other materials at high

temperature. Due to their enormous nature, CNTs have taken the place of other materials in industry (Bian L. and Zhao H., 2014).

2.2.1.2 Applications of CNTs

In general, the application areas of CNTs are as follows (Krishnamurthy G. et al., 2014).

- Hydrogen storage
- Biosensors
- Rechargeable lithium batteries
- Multifunctional composite materials (thermal conductivity, high strength, electrical conductivity)
- Field emission
- Electronic nano devices (diodes, transistors, nanowires, etc.)
- Supercapacitors, organic solar cells and touch screen

2.3 BORON NITRIDE

2.3.1 Characteristics of Boron

Boron is a Group 13 element that has properties which are between metals and non-metals. It is a semiconductor with a wide band gap. Chemically it is closer to silicon than to aluminum, gallium, indium, and thallium. Boron doesn't exist in nature in elemental form. It can be obtained in the environment through release into air, soil and water through weathering. Elemental boron is as hard as diamond crystals.

40-50% of the boron consumption is used in construction of glass and ceramic. 20-30% of the world consumption of boron compounds is employed in the manufacture of bleaching and cleaning powder. 5-10% of them are consumed as fertilizer in agriculture. The remaining 25% is utilized in various industries. Chemical, paper, textile, cement industry, leatherwork, photography, pharmacy, production of fire-resistant material, production of steel, construction of antifreeze are the examples of main application areas.

2.3.2 Boron Nitride (BN)

BN is a chemical compound consisting of equal number of boron and nitrogen atoms. BN doesn't exist in nature and is therefore produced synthetically from boric acid or boron trioxide. Boron nitride is insoluble in usual acids, but is soluble in alkaline molten salts and nitrides. Nowadays, it is constructed largely by reacting boron trioxide or boric acid with ammonia (or sometimes urea) in the atmosphere of nitrogen.

BN has a great potential in nanotechnology (Vel L. et al., 1991). Because of excellent thermal and chemical stability, BN ceramics are traditionally used as parts of high-temperature equipment (Sasaki O. and Ohta H., 1986). BN is a good lubricant and abrasive, and it has a high thermal conductivity, high electrical resistance, and high temperature resistance (Mishima O. et al., 1987). The common structures of the BN are the hexagonal (hBN) and cubic (cBN) crystal forms (Cheewawuttipong W. et al., 2013).

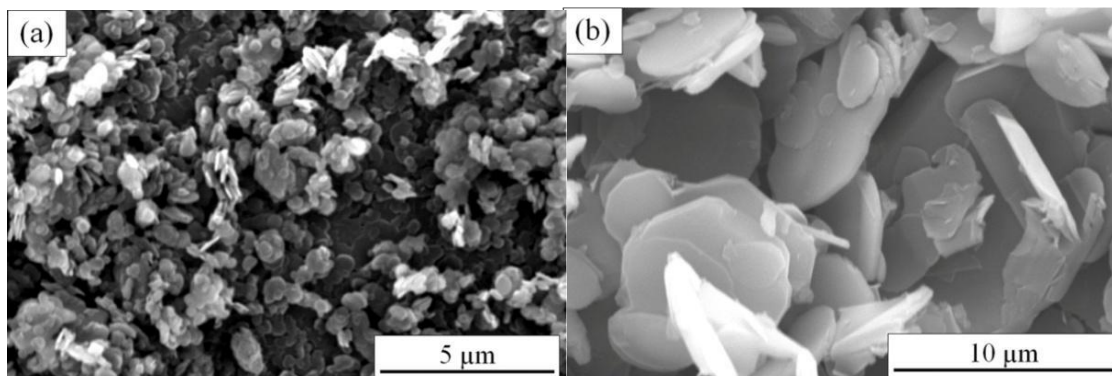


Figure 2.6 (a) BN particles, size 1-2 μm , (b) BN particles, size 7-10 μm . (Cheewawuttipong W. et al., 2013)

2.3.3 Hexagonal Boron Nitride (h-BN)

Atomic structure of a h-BN mimics the graphite, is alumina-like in appearance, white in color, non-toxic and is a slippery material. The h-BN crystal structure is similar to graphite, but it is different from graphite because it is white and has high electrical resistance.

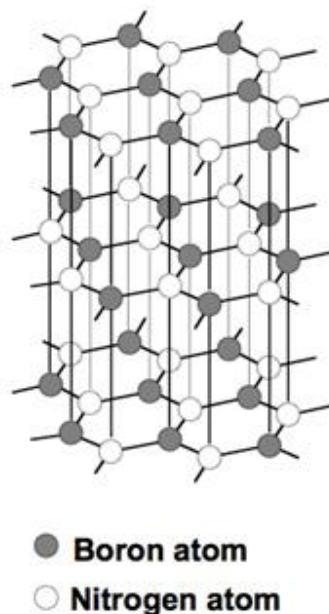


Figure 2.7 Hexagonal form of BN (www.nims.go)

h-BN is an inert material, does not undergo chemical reactions and is not toxic. It is resistant to high temperatures. h-BN is a material which can be used in the normal atmosphere up to 1000°C, in the vacuum environment up to 1400°C, in an argon atmosphere up to 2000°C, in the atmosphere of nitrogen up to 2400 °C. In addition to being stable against thermal shock, h-BN has an excellent electrical insulation, as well as the thermal conductivity of copper and has the capability to reflect UV rays, and has excellent lubricity as well (Kostoglou N. et al., 2014), (Steinborn C. et al., 2013).

2.4 BORON NITRIDE NANOTUBES (BNNTs)

BN is a chemical compound, formed by equal number of boron and nitrogen atoms. BN structures have great potential in nanotechnology and exist in various crystalline forms. One of the forms of BN structure is the BNNT (Chopra N.G. et al., 1995).

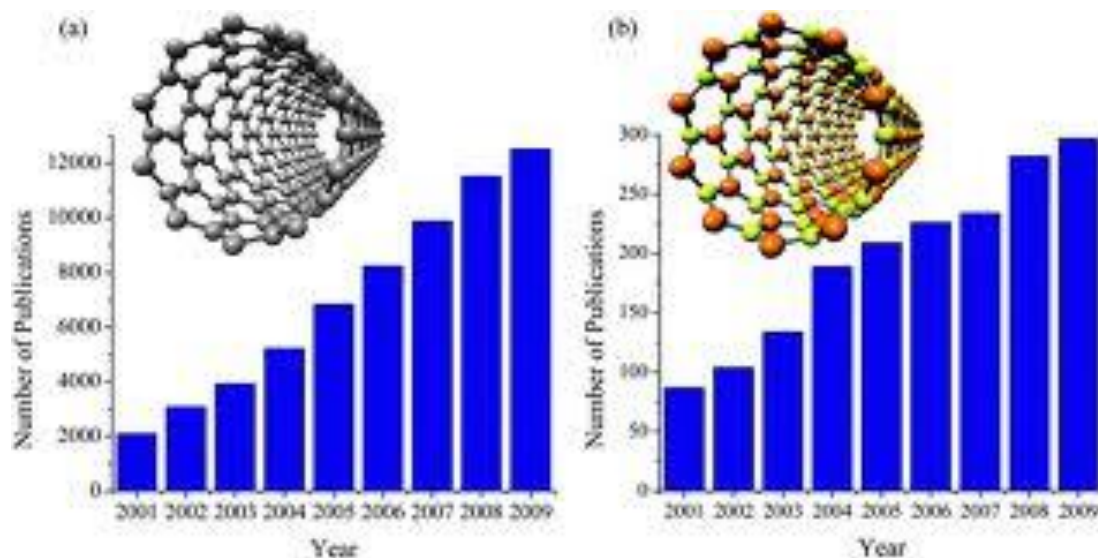


Figure 2.8 The number of publications on (a) CNTs, and (b) BNNTs (based on the ISI Web of Knowledge) (Yap Y.K. et al., 2010).

BNNTs were theoretically proposed (Akdim B. et al., 2003) and observed experimentally (Cumings J. and Zettl A., 2000). BNNTs have the same atomic structure as CNTs. However, the properties of BNNTs are very different from CNTs. So far there have been many studies regarding BNNTs and CNTs, the associated number of publications is given in Figure 2.8. A BNNT is a structure with a certain wide band gap which is independent on the number of tube walls (Blase X. et al., 1994). However CNTs can be metallic or semiconducting. Furthermore, a layered BN structure is much more thermally and chemically stable than a graphitic carbon structure. BNNTs are more resistant to oxidation than CNTs (Wang J. et al., 2009).

Experimental observations revealed that BNNTs in general have the following physical properties (Yap Y.K. et al., 2010):

- stable wide band gap
- superb mechanical strength
- high thermal conductivity
- ultra-violet light emission
- resistant to oxidation

2.4.1 Application Areas of BNNTs

BNNTs are the structures which can be the basis for industry, technology, health and in many other areas and used in revolutionary of materials and processes:

- Due to the having unique physical, chemical, thermal and electronic properties, BNNTs offer many potential uses in technological field.
- BNNTs can be used as hydrogen storage (Zhang Z.W. et al., 2012).
- Because of insulating property, BNNTs can be used as insulating nanotubes.
- They are unique materials which can be used in nano electronic devices due to the uniform band openings.
- Ultra-light aerospace structures can be made using BNNTs which have the properties of unprecedented strength even at high temperatures.
- BNNTs can be used in cancer therapy (Chen X. et al., 2009).
- BNNTs can be used in sports equipments due to their weight, strength and durability.

2.4.2 Synthesis Methods of BNNTs

There are many synthesis methods concerning the production of BNNTs. Some of useful methods are given below (Govindaraju N. and Singh R.N., 2013):

- Arc discharge (2000 °C)
- Laser ablation (1200 °C)
- CVD (Chemical Vapor Deposition) (1200 °C)

Figure 2.9 illustrates transmission electron microscopy (TEM) image of BNNTs grown at NASA. BNNTs can be produced through the above techniques. However, there are some difficulties:

- low efficiency
- High temperature is needed
- Suitable catalysts may not be found

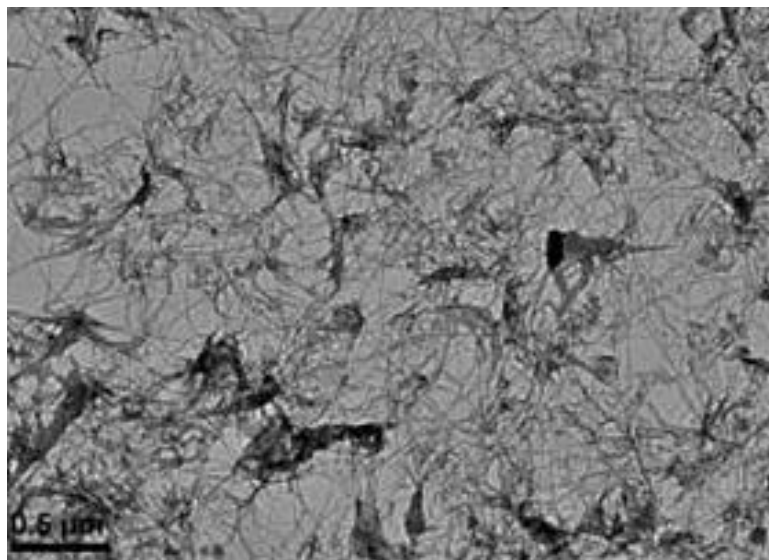


Figure 2.9 Representative TEM image of BNNTs grown at NASA Langley Research Center (LaRC) (Boron Nitride Nanotube: Synthesis and Applications, ntrs.nasa.gov)

2.4.3 Properties of BNNTs

In contrast to CNTs, BNNTs are not good electrical conductors, thereby making the measurement of physical properties of these materials is very challenging. Nevertheless, significant research has been performed on elucidating the fundamental physical properties of BNNTs. Some properties of BNNTs compared to CNTs are presented in Table 2.1. A few important physical properties of BNNTs are described below.

Table 2.1 Comparison of BNNTs and CNTs (Zhi C. et al., 2010).

	BNNTs	CNTs
Mechanical properties (Young's modulus)	1.18 TPa	1.33 TPa
Electrical properties	Always semiconducting with a wide band gap	Metallic or semiconducting
Thermal oxidation resistance	Stable up to 800 °C in air	Stable up to 500 to 700 °C in air
Optical properties	Applicable in the deep-UV	Applicable in the near-IR
Color	Gray	Black
Surface morphology	Corrugated	Smooth

2.4.3.1 Mechanical Properties of BNNTs

BNNTs have an unusual stiffness, with a Young's modulus of 1.2 TPa (Wei X. et al., 2010). This is comparable to the Young's modulus of diamond (~1,000 GPa). Because of this they are promising for reinforcement of polymeric composites and ceramics. These lead to applications in lighter, faster and inexpensive transportation, moreover lightweight armors (Griebel M. and Hamaekers J., 2006). The tensile strength of the BNNTs can vary depending on aspect ratio in terms of tube diameter and length. A maximum value of approximately 33 GPa was recorded (Zheng M. et al., 2013).

Researchers have been working on possible applications of BNNTs, which are as strong as light materials. Such materials may be particularly useful for spacecraft. If the body of a spacecraft is made from BNNTs materials, the boron atoms can absorb neutrons from the solar wind and save the crew and electronic devices.

2.4.3.2 Electrical Properties of BNNTs

BNNTs were discovered in 1995 (Chopra N.G. et al., 1995). So far, there have been much more research into applications for CNTs than for BNNTs; yet researchers are processing in taking advantage of the benefits that BNNTs have. Scientists in nanotechnology engaged in research on BNNTs due to the fact that they have semiconducting properties and, thus, they are very useful in electronics (Radosavljević M. et al., 2003).

BNNTs have a great potential in nanotechnology. BNNTs have a similar structure as CNTs, while their electronic properties are quite different from CNTs, however they exhibit only semiconducting properties independent of their chirality and diameter with wide band gaps ranging up to 5.5 eV (Oku T et al., 2008). BNNTs have more stable electrical properties than CNTs have. BNNTs can be used as the transistor channel instead of CNTs.

The wide band gap makes BNNTs promising materials for applications in nanoelectronics and optoelectronics. If their band gap can be controlled like a normal semiconductor through a regular mechanism, their ranges of application would be greatly extended (Jhia S.H. et al., 2005). It was shown that the band structures of

BNNTs can be strongly modified and band gap closing had been predicted (Zhi C. et al., 2005).

2.4.3.3 Thermal Conductivity of BNNTs

BNNTs have many interesting properties. One of them is the thermal conductivity. BNNTs have a high thermal conductivity. It is theoretically 300 W/mK (Zhi C. et al., 2010). They are predicted to have a high thermal conductivity at low temperatures. This makes BNNTs useful for applications in nanoelectronics due to the demand for heat dissipation in this field (Mashreghi A., 2012).

The thermal conductivity of BNNTs is similar to the CNTs because of the same phonon dispersion relation, although h-BN has a lower thermal conductivity than graphite. BNNTs can survive up to 1100 °C in air. In fact, because of their excellent thermal and chemical stability, BN materials have been used as high-temperature ceramic for years.

2.4.3.4 Thermal Oxidation Resistance of BNNTs

BNNTs have a similar structure as CNTs but were found to exhibit significant resistance to oxidation at high temperatures. Thermogravimetric analysis shows a starting temperature for oxidation of BNNTs of 800 °C compared with only 400 °C for CNTs under the same conditions (Chen Y. et al., 2004). This high level of resistance to oxidation can make applications of BNNTs to work at high temperatures.

CNTs are oxidized at 400–500 °C in air and totally burnt out at ~700 °C, on the contrary, the oxidation of BNNTs begins at 650–950 °C and the burning-out happens above 1200 °C (Wang J. et al., 2010).

2.4.3.5 Optical properties of BNNTs

Light emission of BNNTs takes place within a very limited range of the ultraviolet (UV) spectrum, which means they cannot be used in applications in which the emission needs to be produced within a wide range of frequencies. For instance, they cannot be

used in applications requiring visible light. But the researchers have been investigating a solution to overcome this limitation, and trying use of BNNTs in industrial applications (Lahiri D. et al., 2010).

By applying an electric field perpendicular to the BNNTs, it is possible to get emission of light across the whole spectrum from the infrared to the far ultraviolet and to control it in a simple way. The length of these tubular structures is in the micrometers, the diameter is in nanometers. This easy control is available for BNNTs due to their cylindrical geometry (Harigaya K., 2010).

Optical properties of multiwall BNNTs were investigated by means of luminescence and absorption spectroscopes. Cathodoluminescence imaging indicates that BNNTs are highly UV luminescent materials and that the luminescence is located along the nanotube (Zhi C et al., 2010).

2.5 SPINTRONICS

Electrons carrying negative electric charge have spin property. An electron spin is described by its orientation: *spin up* or *spin down*. Conventionally, electrons with spin up and spin down are known as *majority* and *minority* electrons, respectively. The ordinary electronics uses only charge of electrons for storage, processing of information and in manipulating the electrons and neglects the spin property of electrons. However, spintronics employs the spin property of electrons in addition to their charge (Sarma S.D., 2001). This field can be applied in order to develop novel materials in nanotechnology. Spintronics involves the spin unrestricted electron structure properties of nanoscale systems and electronic transport in molecular (and solid state) devices (Pati R. et al., 2003). Spintronics emerged in the 1980s from studies regarding the electron transport phenomena in solid state devices. One of these studies was the observation of spin polarized electron injection from a ferromagnetic metal to a normal metal (Johnson and Silsbee, 1985). Another important one was the discovery of the giant magnetoresistance (Baibich M. N. et al., 1988).

Spintronics intends to find the effective ways of controlling electronic properties of a system through the electron spin. A magnetic field can be utilized to control the spin so that it can be used to provide extra functionality in new generation of electronic devices. In device structures, spintronics deals with injection, detection and manipulation of electron spins. More advanced spintronic technologies are in the early research stages, such as spin field effect transistor (spin FET), which employs the spin in controlling the current flow. Spin FET is one of the best examples for a device structure (Datta S. and Das B., 1990). It consists of two electrodes (source and drain) and a channel (system) between them. Spin FET hasn't yet been applied in technology.

Spintronics leads to revolutionary advances in the next generation of electronics, for instance, logics with extremely low power, enhanced functionality of devices, ultra fast, high dense memory devices, smaller device size as well as faster operation (Wolf S.A. et al., 2001).

CHAPTER 3

THE METHOD

3.1 ATOMISTIX TOOLKIT (ATK)

Atomistix Toolkit (ATK) is a software for modeling of atomic size and simulation of nanosystems (www.quantumwise.com). ATK can be employed to investigate both electronic transport and magnetic properties of nanoscale systems in the presence of spin. One can examine molecules, bulk and device structures. ATK is based on DFT which can provide to model and analyze the behavior of nanoscale structures.

Basic features of ATK briefly stated as follows;

- ATK is ability to calculate the electronic transport properties of systems under an applied bias voltage.
- ATK can optimize the geometry of the systems in the atomic scale.
- ATK can simulate the electrical, optical and mechanical properties of nano devices on the atomic scale modeling.
- ATK can perform calculations for many systems including molecular, bulk and two probe systems.
- Most physical quantities like spin dependent transmission, density of states, current-voltage characteristics, energy spectra, wave functions, electron densities, atomic forces, effective potential can be obtained.

It involves the numerical methods carrying out *first-principles* calculations. ATK solves the quantum mechanical equations and simulates the experimental works. In addition it yields data about spin unrestricted electronic structure and transport properties of nanoscale materials.

3.2 DENSITY FUNCTIONAL THEORY (DFT)

The DFT is one of the most efficient and promising methods for considering systems consisting of many particles (Hohenberg P. and Kohn W., 1964). DFT is a good and successful theory in solving, understanding and simulating of complex quantum mechanical systems. DFT based computational codes employing *first principles* are used in practice to investigate the electronic structure, magnetic and transport properties of various systems.

The DFT is based on the theorems developed by Hohenberg and Kohn (H-K) (Hohenberg P. and Kohn W., 1964). In 1964 Hohenberg and Kohn developed a theorem which states that the exact ground-state energy is a functional (a function of a function) of the exact ground-state one-particle density. After that, DFT has been very useful method for theoretical calculations in solid state physics. According to the fundamental theorems obtained by Hohenberg and Kohn, the electron density carries all the information one might need to determine any property of the electron system. The first H-K theorem showed that the ground state properties of a many electron system can be determined by the electron density. The second H-K theorem describes the energy function of the system and proves that the correct ground state electron density minimizes this energy functional.

In the past 40 years, DFT was developed by Kohn and Sham (Kohn W. and Sham L.J., 1965). They have had a great success in explaining the quantum mechanical ground state of electrons in systems of interest in quantum chemistry and solid state physics. The Kohn-Sham equation is the Schrödinger equation of an imaginary system of non-interacting electrons that form the same density as any given system of interacting electrons. This was a great accomplishment towards the approximation to the *exchange correlation functionals*, explained below (Engel E. et al., 1996).

In a system, for a set of interacting electrons moving quantum mechanically in the potential field of a set of atomic nuclei, which are assumed to be static, the solution generally requires to usage of approximations, such as Hartree theory and Hartree-Fock theory. The DFT has become the most useful method for a system consisting of many particles. There is a balance between accuracy and computational cost which depends on the approximations to exchange correlation energy functionals. The usual ones are

Local Density Approximation (LDA) (Jones R.O. and Gunnarsson O., 1989) and *Generalized Gradient Approximation* (GGA) (Perdew J.P. et al., 1992). The corresponding exchange correlation functionals used in DFT calculations are LDA.PZ, GGA.PBE and SGGA.PBE. LDA.PZ is the local density approximation with the Perdew-Zunger parametrization (Perdew J.P. and Zunger A., 1981) of the correlation energy of a homogeneous electron gas calculated by Ceperley-Alder (Ceperley D.M. and Alder B.J., 1980). GGA.PBE is Perdew-Burke-Ernzerhof parametrization of the generalized gradient approximation. SGGA.PBE employs the GGA.PBE for spin unrestricted calculations.

In LDA, the energy functional depends on the electron density at any position (Jones R.O. and Gunnarsson O., 1989). In LDA, this functional is defined as follows:

$$E_{xc}^{LDA}[n] = \int \varepsilon_{xc}[n(r)]n(r)dr \quad (3.1)$$

where E_{xc} is the exchange correlation energy (energy functional), ε_{xc} stands for energy per particle and $n(r)$ represents the electron density. In the LDA, ε_{xc} is supposed to be homogenous at every point in the system.

In GGA, the gradient of the electron density at the same position is also included (Perdew J.P. et al., 1992). In GGA, exchange correlation energy is described by

$$E_{xc}^{GGA}[n] = \int f[n(r), \nabla n(r)]n(r)dr \quad (3.2)$$

where $f[n(r), \nabla n(r)]$ is a functional, which is a function of both electron density and its gradient. Reasonable results were achieved using the GGA, especially, for molecular geometries and ground state energies.

The wave function Ψ indicates all information about the system in quantum mechanics. This wave function is employed in Schrödinger's equation. For a single electron moving under an external potential $V_{\text{ext}}(r)$

$$\left[-\frac{\hbar^2 \nabla^2}{2m} + V_{\text{ext}}(r) \right] \Psi(r) = E \Psi(r) \quad (3.3)$$

where E is the energy and m denotes the effective mass. For a system consisting of N electrons (many-body problem), Schrödinger's equation is given by the following equation:

$$\left[\sum_i^N \left(-\frac{\hbar^2 \nabla_i^2}{2m} + V_{\text{ext}}(r) \right) + \sum_{i < j} U(r_i, r_j) \right] \Psi(r_1, r_2, \dots, r_N) = E \Psi(r_1, r_2, \dots, r_N) \quad (3.4)$$

Here, $U(r_i, r_j)$ indicates the electron electron interaction and $\Psi(r_1, r_2, \dots, r_N)$ is the many-body wave function. Solving this equation exactly is impossible and therefore we need some approximations. The most probable solution for this type of problem is to apply the ground state electron density $n(r)$. $n(r)$ is used for defining many electron system and in calculating ground state energy.

The H-K theorem noted that the $n(r)$ can be used in place of potential as a basis function which uniquely describes the system. The ground state $n(r)$ defines the external potential $V_{\text{ext}}(r)$. The ground state energy is minimized by the ground state charge density. The energy functional $E(n(r))$, function of the $n(r)$, can be written in terms of $V_{\text{ext}}(r)$ as

$$E[n(r)] = \int V_{\text{ext}}(r) n(r) dr + F[n(r)] \quad (3.5)$$

where $F[\mathbf{n}]$ denotes an unknown functional independent of the $V_{ext}(r)$. The relationship between $n(r)$ and $\Psi(r_1, r_2, \dots, r_N)$ is given by

$$n(r) = N \int |\Psi(r_1, r_2, \dots, r_N)|^2 dr_2 \dots dr_N \quad (3.6)$$

The total energy functional is defined by

$$E[\mathbf{n}] = T[\mathbf{n}] + E^{xc}[\mathbf{n}] + E^H[\mathbf{n}] + E^{ext}[\mathbf{n}] \quad (3.7)$$

where $E^{xc}[\mathbf{n}]$ represents the exchange correlation energy, $E^H[\mathbf{n}]$ indicates the Hartree energy, $E^{ext}[\mathbf{n}]$ shows the interaction energy concerning the *pseudo* potential ions and other electrostatic external potentials. $T[\mathbf{n}]$ is the kinetic energy of the Kohn-Sham orbital expressed by the following equation

$$T[\mathbf{n}] = \sum_{\alpha} \left\langle \Psi_{\alpha} \left| -\frac{\hbar}{2m} \nabla^2 \right| \Psi_{\alpha} \right\rangle f\left(\frac{\varepsilon_{\alpha} - \varepsilon_F}{kT}\right) \quad (3.8)$$

Differentiating the total energy $E[\mathbf{n}]$ with respect to the ionic coordinate of any atom at a position results in certain forces which are the balance forces between the atoms in the system.

3.3 GREEN'S FUNCTION (GF) FORMALISM

GF formalism is in general employed in the absence of bias, that is when the system is in equilibrium. The single particle GF operator $\hat{G}(E)$ of a system can be explained by the solution of the operator equation,

$$[E - \hat{H}]\hat{G}(E) = 1 \quad (3.9)$$

Thus, $\hat{G}(E)$ is described as $\hat{G}(E) = (E - \hat{H})^{-1}$. The GF is a wave function at position x resulting from a unit excitation at x' . In terms of position, the equation above can be rewritten as

$$[E - H(x)]G(x, x', E) = \delta(x - x') \quad (3.10)$$

where the GF is described as

$$G(x, x', E) = \langle x | \hat{G}(E) | x' \rangle \quad (3.11)$$

GF can be regarded as a source of an excitation. From Equation (3.10), GF is not well determined for an amount of E corresponding to the eigenvalues of the Hamiltonian. Because of this, one must introduce an extra parameter (η), which gives retarded (G^+) and advanced (G^-) GFs. In this case, Equation (3.10) is rewritten as

$$[E \pm i\eta - H(x)]G^\pm(x, x', E) = \delta(x - x') \quad (3.12)$$

3.4 NON EQUILIBRIUM GREEN'S FUNCTION (NEGF) FORMALISM

The NEGF method is usually used for calculating the charge densities and the current through the nanoscale systems under a finite bias, implying the systems in non equilibrium. The bias is applied by means of left and right electrodes. The system is located between them, forming a *two probe system* or *device* structure. In the NEGF method, the effect of the left and right electrodes is taken into account through the associated *self-energies* and the details of the central region, where the system is inserted, is given by the Hamiltonian as follows:

$$G(E) = \lim_{\eta \rightarrow 0} [(E + i\eta) - H_s - \Sigma_L - \Sigma_R]^{-1} \quad (3.13)$$

where Σ_L and Σ_R represent the self energy for the left and right electrodes, respectively. Self energies involve information about the electronic structure of the electrodes and their contact to the central region. As stated, a two probe system (or device) consists of three main parts: The central (or scattering) region, where the system is placed, left electrode (source) and right electrode (drain). It is shown in Figure 3.1.

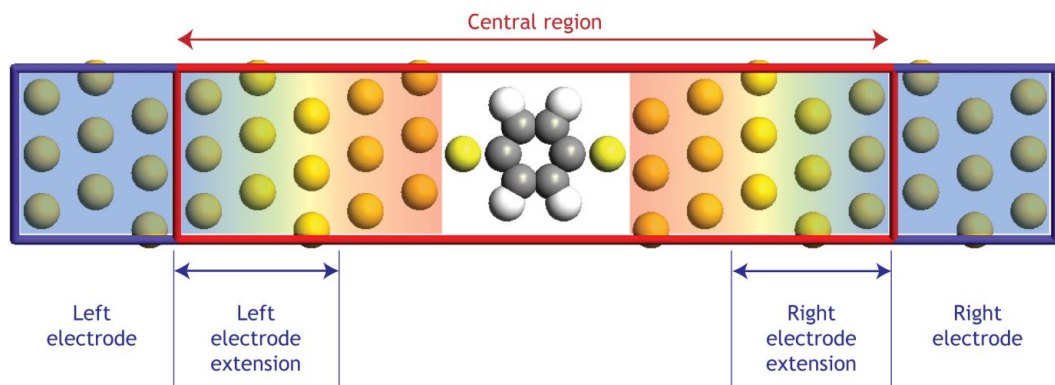


Figure 3.1. Geometry of a device system consisting of a central region and two electrodes (www.quantumwise.com)

CHAPTER 4

CALCULATIONS AND RESULTS

4.1 SYSTEMS AND DFT PARAMETERS

We have investigated both pure and doped BNNTs with distinct radii. In this thesis, we have mainly focused on spin unrestricted electronic structure properties of these systems, using *first principles* through DFT calculations. In the calculations, for the sake of comparison, we have altered some parameters, such as exchange correlation functionals and k-points sampling. The chiral vector, denoted by (n, m) , defines the tube helicity of the BNNTs. $(n,0)$ gives the zigzag; (n,n) , where, is the armchair; and (n,m) , where, yields the helical BNNT structures. In the present study we only considered zigzag BNNTs by modifying the n , giving rise to a change in radius and, hence, to that in number of atoms. We basically investigated $(4,0)$, $(6,0)$ and $(8,0)$ zigzag BNNTs, which are represented by BN-4, BN-6 and BN-8, respectively in this thesis. The corresponding radii of BN-4, BN-6 and BN-8 are 1.60 Å, 2.38 Å and 3.16 Å, respectively obtained for optimized structures.

We have constructed the BNNTs such that they are periodic (infinite) along the z axis. Therefore they are finite with a certain diameter along x and y axes. For these one dimensional systems, thus, k -points were taken as $(1,1)$ for the transverse axes and 21, 51 and 99 were considered for the z axis to see the effect of it on the band gap (E_g) and spectra. In order to mimic the realistic situations and to be comparable with experimental results, before performing the calculations, the structures that we constructed were optimized or relaxed. The atomic positions were relaxed employing the force tolerance of 0.05 eV/Å. The optimization gives 1.45 Å as the bond length of B-N atoms in the pure BNNTs. DFT calculations were performed through the exchange

correlation functional GGA.PBE (or SGGA.PBE for the spin unrestricted calculations). Double zeta polarized basis set was employed for all atoms in the supercell.

We have intended to examine the possible modifications in spin unrestricted electronic structure properties of BNNTs, mentioned above, in terms of radius and dopant type. In addition, the influence of location of dopants in the BNNT was also explored. In the BNNT structures, we have involved various transition metal atoms like cobalt (Co), chromium (Cr), and nickel (Ni) as dopants in order to observe possible spin unrestricted behavior or emerging magnetism. When dopants are included, the structure was repeated 3 times (to enhance the size of the unitcell along tube axis) along the z axis to have sufficient number of atoms in the supercell.

4.2 PURE BNNTs

In general we have performed both spin restricted and unrestricted first principles calculations on pure and doped BNNTs. In order to extract relevant electronic properties, we have obtained E_g and density of states (DOS) spectra. Moreover the magnetic properties were also examined through the Mulliken population (Mulliken R.S., 1955) for doped structures. The Mulliken population analysis can yield the magnetic moment induced in a system. The Mulliken analysis is related to charge population. It gives, in general, the number of electrons for each atom in the system. In spin unrestricted cases, it gives rise spin up and down populations or results in spin charge density magnetization: spin up charge density minus spin down charge density. Hence, from this data one is able to get the corresponding magnetic moment in a similar manner.

In the following we present the DOS spectra and band gap results and give necessary explanations for each system.

4.2.1 System BN-4

The zigzag BN-4 structure is illustrated in Figure 4.1 where both base (top or bottom) and side views are shown. It is infinite along the tube or z axis (axis in yellow in Figure 4.1). The number of atoms in the unit cell, length of which along z is 4.34 Å, is 16. The radius of BN-4 becomes 1.60 Å for an optimized structure.

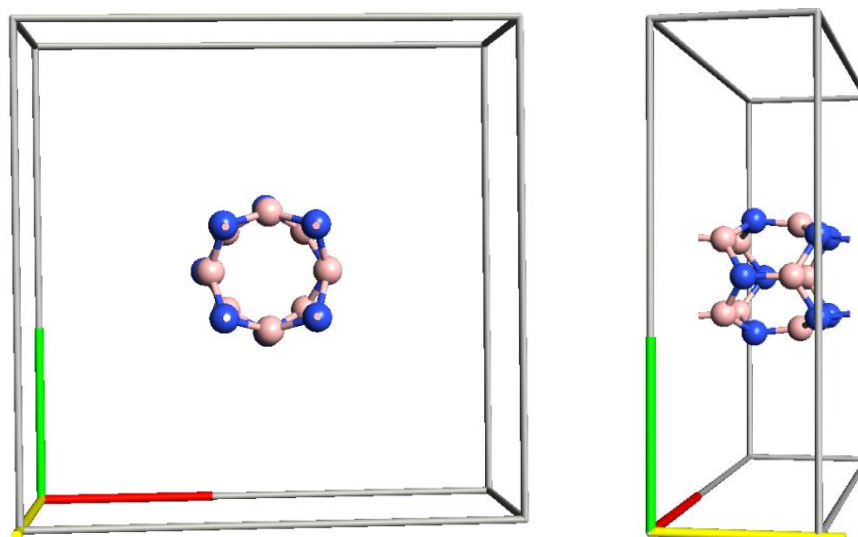


Figure 4.1 Base and side views of zigzag BN-4 in the unit cell where the axis in yellow denotes the z (tube) axis. B and N atoms are shown in rose and blue, respectively.

The spin independent DOS spectrum for pure BN-4 is illustrated in Figure 4.2. DOS implies the electronic structure behavior and using this spectrum one can obtain the E_g of a system. For BN-4, E_g was found as 1.44 eV. In an earlier work, it was obtained as 1.80 eV (Zhang Z. et al., 2009. They reported the stability and electronic structures of the BNNTs with diameters below 4 Å by semi-empirical quantum mechanical molecular dynamics simulations and *ab initio* calculations. It was obtained that, these small BNNTs can be semiconductor or remain insulator depending on their chirality). The zero DOS in the vicinity of the Fermi level (E_F) yields the band gap of a semiconductor or insulator. In the present work E_F is set to zero. In Figure 4.2, we see that there are sharp peaks at energies $E = -0.75$ eV, -0.88 eV and 0.69 eV in DOS, just above and below the E_g . The energy states around the E_F in DOS spectrum characterize the electronic behavior of the system. We observed a smooth variation at positive energies (conduction band) and more sharp peaks together with more oscillations at particular negative energies (valence band). The suppressed and well defined peaks give the (both spin unrestricted and restricted) electronic transport feature of a system. A zero DOS at particular energies in the spectrum means that the electron states are not available at these energies.

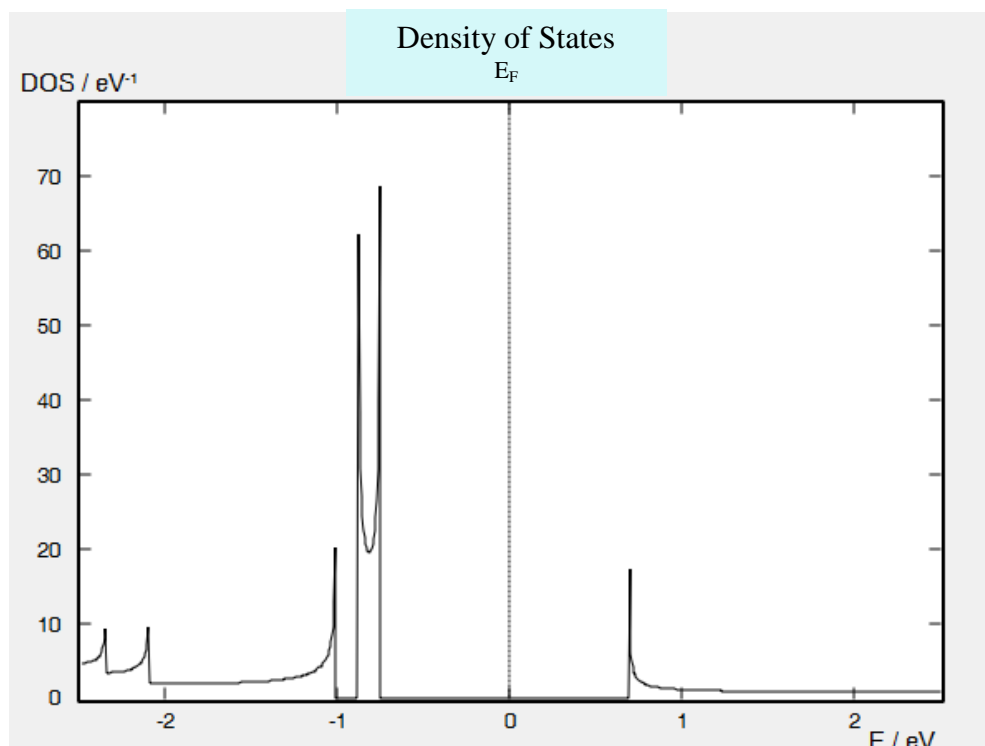


Figure 4.2 DOS spectrum for zigzag BN-4 in the absence of spin.

The DOS spectrum shown in Figure 4.2 was obtained using k-points (1,1,21). To make sure the accuracy of the calculations, we have modified the number of k-points for the tube axis. It was changed to 51 and 99 for a specific system to observe the effect of k-points on the results. According to the results, we found that the relevant quantities were independent of k-points from (1,1,21) to (1,1,99). Hence, in the calculations we have employed (1,1,21) since increasing it leads to the both memory and time consuming DFT calculations.

4.2.2 System BN-6

Base view of zigzag BN-6 structure is shown in Figure 4.3. It is infinite along the tube axis and the number of atoms is 24 in the unit cell. While the lattice parameter along z is fixed (4.34 Å), the radius, now, becomes 2.38 Å for the optimized structure.

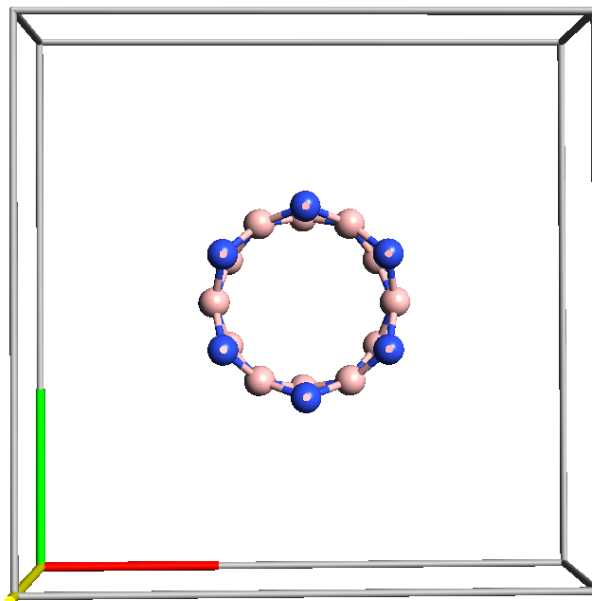


Figure 4.3 Base view of zigzag BN-6 in the unit cell. B and N atoms are shown in rose and blue, respectively.

The spin independent DOS spectrum for pure BN-6 is given in Figure 4.4. From the DOS variation around the E_F , E_g was obtained as 2.68 eV in the absence of spin. It was calculated to be 4.42 eV in an earlier study (Rimola A. and Sodupe M., 2014, where calculations were carried out using the periodic *ab-initio* code and geometry optimizations were performed using the density functional method). In Figure 4.4, we observe that the abrupt variations in DOS exist at energies -1.91 eV and 0.77 eV close to E_g . We noticed that a smooth variation at positive energies and more sharp peaks at negative energies in DOS persist for BN-6 as seen in Figure 4.4.

The DOS spectrum for pure BN-6, as an example, in the presence spin is also given in Figure 4.5. An exact spin symmetric DOS oscillation was observed, implying no spin dependence, as illustrated in Figure 4.5. Hence, there is no change in the E_g , which is 2.68 eV for both spin orientations, and the E_g becomes independent of spin direction. The spin symmetric spectrum means that no spin polarization or magnetization is induced in the absence of transition metals in pure BNNTs. In the presence of spin, the sharp peaks emerge at energies -0.96 eV and 1.72 eV, just above and below the E_g .

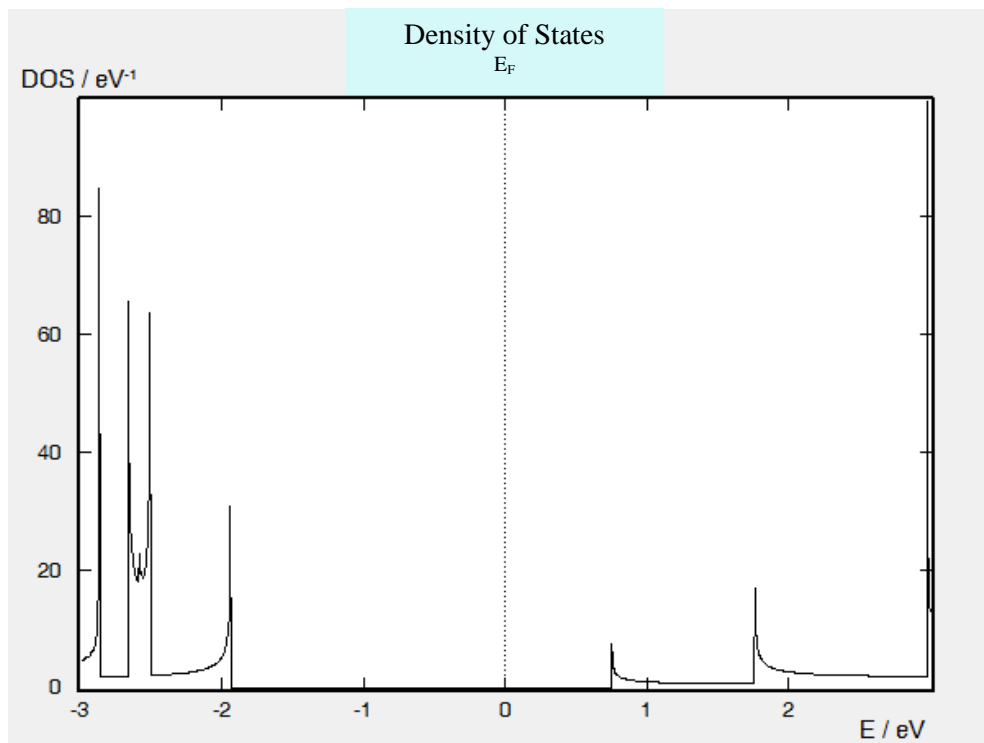


Figure 4.4 DOS spectrum for zigzag BN-6 in the absence of spin.

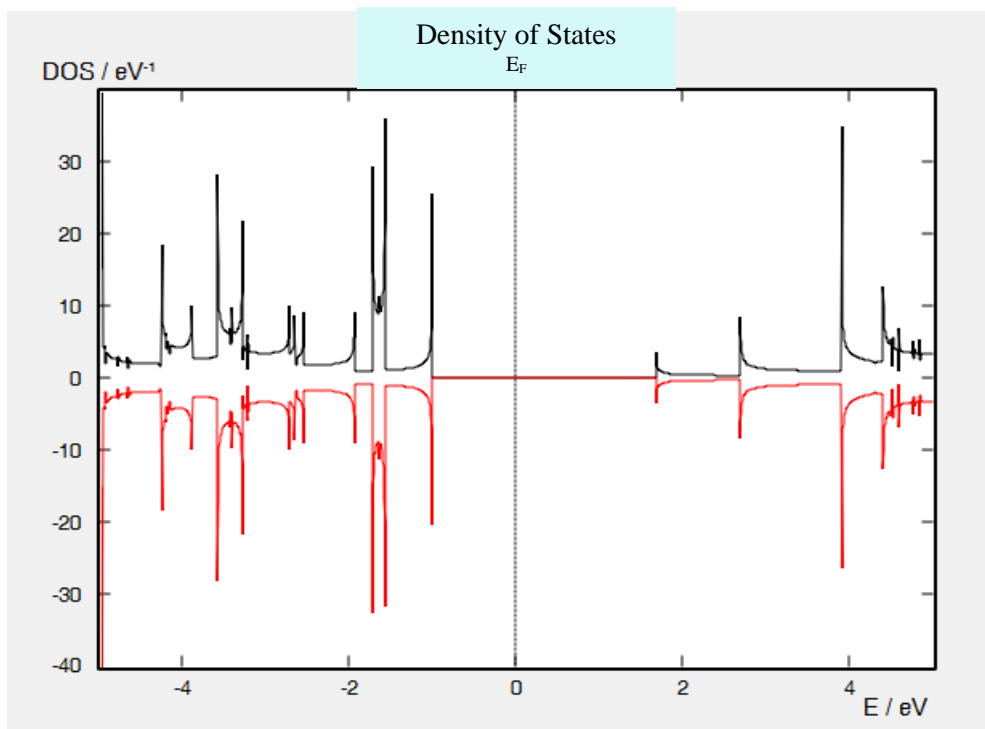


Figure 4.5 DOS spectrum for zigzag BN-6 in the presence of spin.

4.2.3 System BN-8

The zigzag BN-8 structure is displayed in Figure 4.6. This infinite structure along the z axis shown in Figure 4.6 has 32 atoms in the unit cell. The radius of BN-8 was found to be 3.16 Å for the optimized structure.

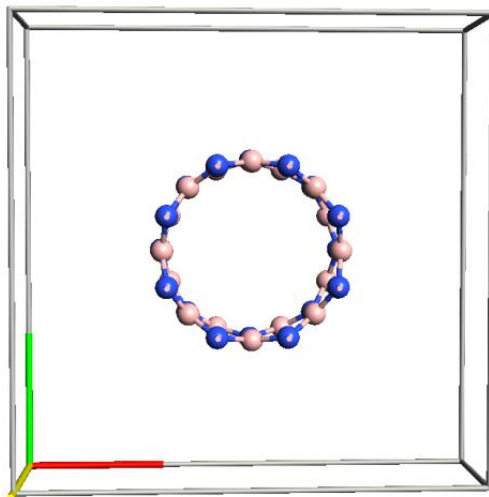


Figure 4.6 Base view of zigzag BN-8 in the unit cell. B and N atoms are shown in rose and blue, respectively.

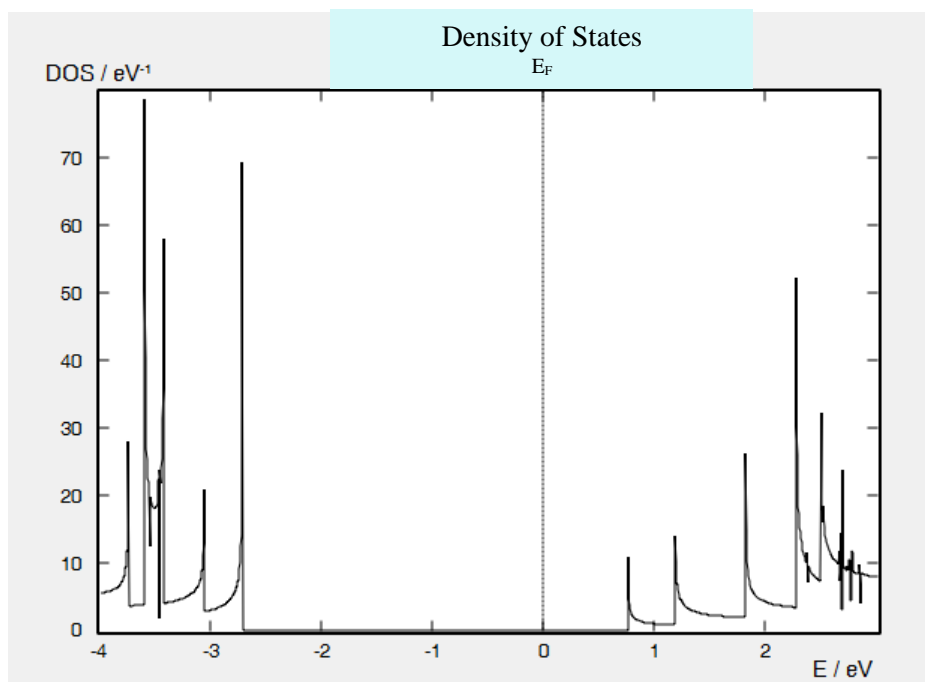


Figure 4.7 DOS for a zigzag BN-8 in the absence of spin.

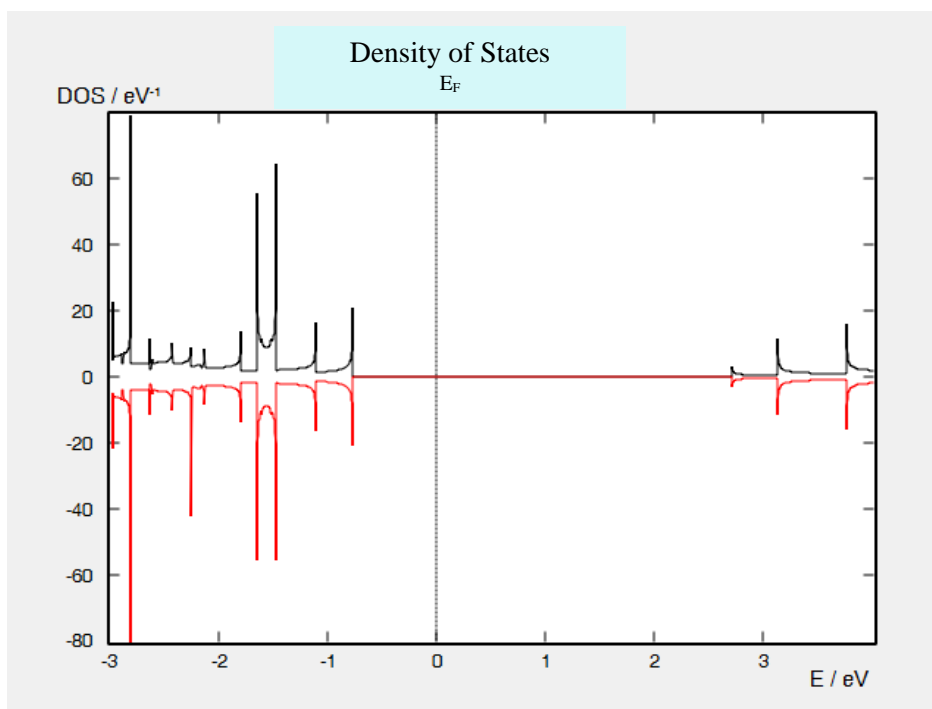


Figure 4.8 DOS for a zigzag BN-8 in the presence of spin.

The spin independent DOS spectrum for pure zigzag BN-8 is shown in Figure 4.7. For this structure, E_g was calculated as 3.47 eV. In the literature the E_g value was stated as 5.63 eV (Esrafil M.D. and Behzadi H., 2012. A DFT study was carried out to investigate the geometry and electronic structure of pristine and C doped (8, 0) single-walled BNNTs). As observed in DOS spectrum in Figure 4.7, unlike the spectra for BN-4 and BN-6, there are more oscillations with sharp peaks in the vicinity of the E_g . The first peaks at negative and positive energies are located at energies -2.75 eV and 0.71 eV. The reason of these extra peaks is due to increase in the number of atoms, yielding more available electronic energy states in the valence and conduction band.

The DOS spectrum for pure BN-8 in the presence of spin was also observed as shown in Figure 4.8. Since no transition metal is doped, as expected, there is no spin asymmetry in the DOS spectrum, yielding spin independent variation. Thus E_g remains fixed (3.47 eV). In this case, the first peaks emerge at energies -0.75 eV in the valence band and 2.71 eV in the conduction band.

In Table 4.1, we present the band gap values of the BNNTs we have examined. It is obvious that the E_g is dependent of radius of a zigzag BNNT.

Table 4.1 Band gap values for zigzag BN-4, BN-6 and BN-8.

System	Radius (Å)	Chiral Vector		E_g (eV)
		n	m	
BN-4	1.60	4	0	1.44
BN-6	2.38	6	0	2.68
BN-8	3.16	8	0	3.47

4.3 DOPED BNNTs

In addition to pure systems, transition metal atom doped BNNTs have also been examined to reveal spin polarization or magnetism which is utilized in the field of spintronics. Thus, we have intended to extract possible spintronic applications of doped BNNTs in novel technology. We have mainly concentrated on low concentration of various dopants like Ni, Co, Cr and Au. To this end, BNNTs mentioned above were repeated 3 times along the z axis, forming a supercell which has now sufficient number of B and N atoms as displayed in Figure 4.9. In this case, the total number of atoms of BN-4, BN-6 and BN-8 structures in the supercell becomes 48, 72 and 96, respectively. In this section we only present the results for doped BN-4 systems, through which we can have a general idea about the effect of dopants in BNNTs on the spin unrestricted electronic behavior.

We have mainly investigated the possible spin dependent changes in the band gaps of doped systems by means of band structure and DOS calculations. The spin unrestricted calculations have been performed through SGGA.PBE exchange correlation functional and k-points (1,1,21). We have mainly examined two situations:

- Spin dependent E_g upon introducing the substitutional transition metal atoms (that is host B atoms are replaced by dopants).

- Examination of the effect of various transition metals on the spin dependent E_g .

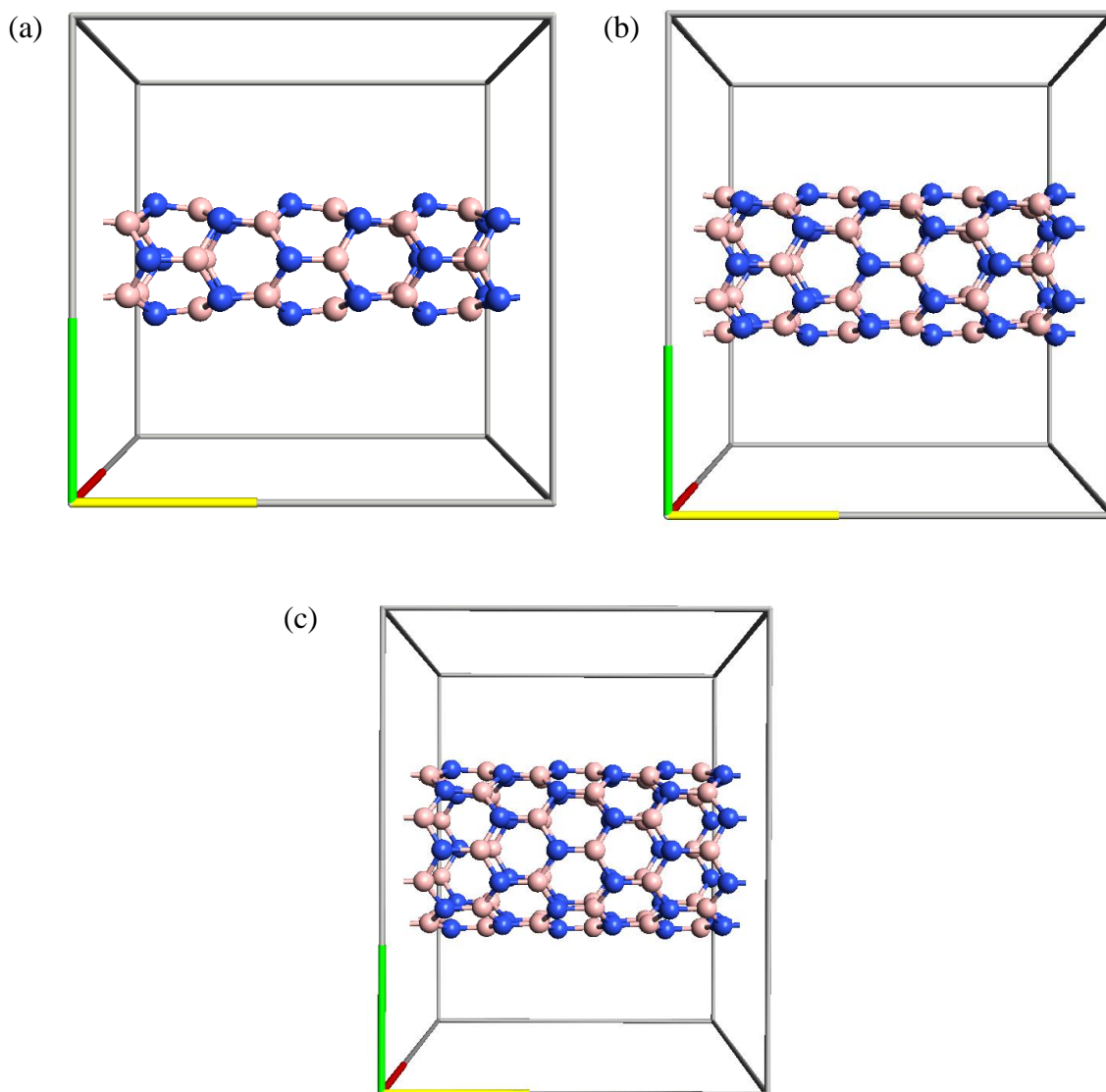


Figure 4.9 Side views of (a) BN-4, (b) BN-6 and (c) BN-8, repeated 3 times along the z axis.

After replacing the B atoms by the transition metal atoms, the initial doped systems were optimized. In this way, the actual bond lengths between a dopant and its nearest-neighbors (N atoms) have been determined. In doped systems, in average, the bond length between B and N atoms was 1.47 \AA . Replacing a single B atom by a transition metal atom (substitutional dopant) corresponds to 2.1% concentration of dopants in the supercell. In the following, we present the doped BN-4 systems, where only a single B

atom is replaced by a transition metal atom. In addition to DOS spectra and E_g values, the induced magnetic moment, emerging due to the transition metal atom, in the system is also presented.

4.3.1 Co Doped BN-4

The substitutional Co doped optimized BN-4 system is shown in Figure 4.10. It must be noted that crucial displacements around the Co atom have been occurred during the relaxation of the geometry where only a single B atom is replaced by a Co atom. In a Co doped BN-4, the bond lengths between Co and three N atoms were 1.81 Å (the distance along tube) and 1.78 Å. The emerging magnetic moment on each atom is not fixed but depends on whether the host atoms are close to transition metal atom. Here we only give the average value. The induced or emerging average magnetic moment per atom in the Co doped BN-4 was found to be $0.036 \mu_B$ (Bohr magnetron).

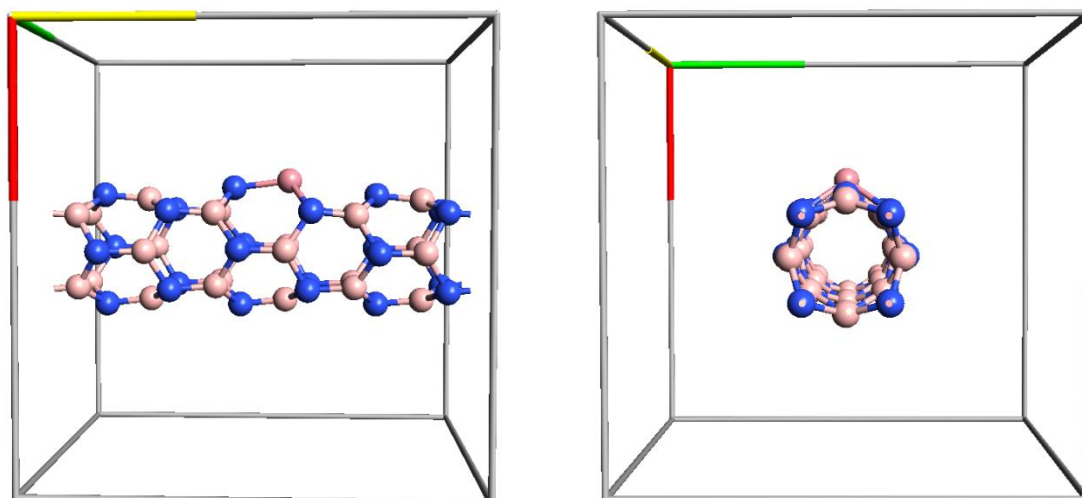


Figure 4.10 Side and base views of zigzag Co doped BN-4 in the supercell where the axis in yellow denotes the z (tube) axis. B, N and Co atoms are shown in rose, blue and dark pink, respectively.

The spin unrestricted DOS spectrum of Co doped BN-4 is illustrated in Figure 4.11 which displays the associated E_g for majority (spin up) and minority (spin down) spins. Majority and minority E_g were found as 0.73 eV and 0.14 eV, respectively (Xie Y. et al., 2012). In order to explore the possible novel applications of BNNT, they

investigated the structural, magnetic and electronic properties of CO and NO molecules adsorption on transition metals such as V, Cr, Mn, Fe, Co or Ni doped (8,0) BNNT using first-principle calculations with DFT under GGA. The results indicated that BNNT may be functionalized when a substitution transition metal is present in the tube wall, and it may be a potential material for nanodevice applications). For the sake of clarity, majority and minority DOS spectra are displayed by black (positive) and red (negative) variations, respectively. The spin asymmetric DOS variation is obvious in Figure 4.11 where two huge abrupt majority peaks and negligible minority peaks are seen in the vicinity of the E_F . At some certain energies contribution of one of the spin orientations to the DOS dominates the other one. We can definitely infer that, around the E_F , the main contribution to the electronic properties comes from majority spins as the corresponding DOS becomes as large as 550 eV^{-1} . Away from the E_F , in the energy interval from -1 eV to 1 eV, minority spins become dominant. Therefore, from the obtained DOS spectra and spin dependent E_g , we can state that introducing a single Co atom can result in a significant change in the electronic structure behavior of a BNNT.

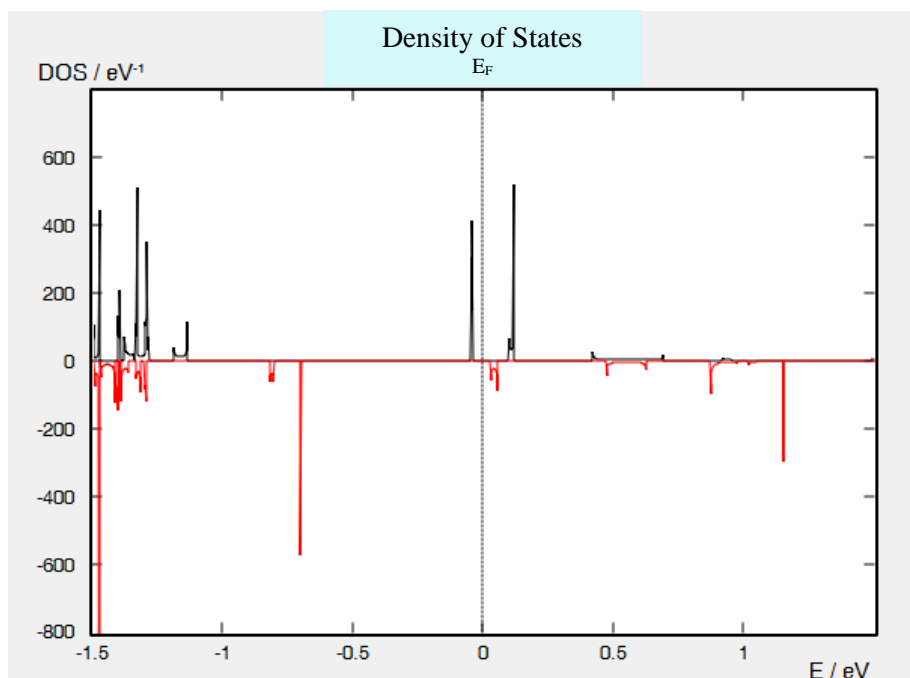


Figure 4.11 DOS spectrum of zigzag Co doped BN-4 in the presence of spin. Black (positive) and red (negative) variations indicate the majority and minority DOS, respectively.

4.3.2 Cr Doped BN-4

We have intended to observe the modification in the spin unrestricted behavior upon introducing a single Cr atom. The optimized Cr doped BN-4 system, where a single B atom has been replaced by Cr atom, is shown in Figure 4.12. In relaxed system, the bond lengths between the Cr atom and its nearest-neighbor N atoms were 1.78 Å (the distance along the tube) and 1.76 Å. In the Cr doped BN-4, the induced average magnetic moment per atom was obtained as 0.063 μ_B .

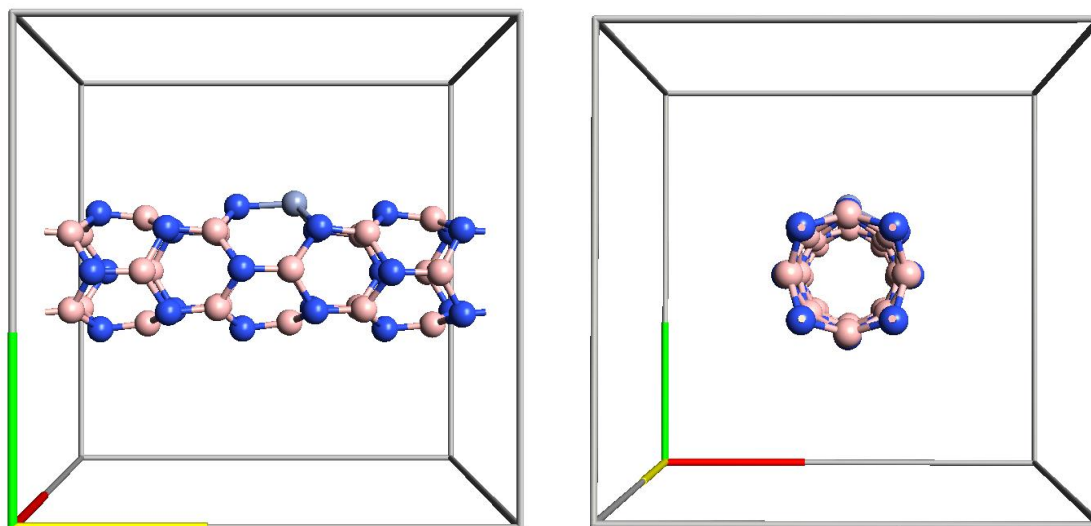


Figure 4.12. Side and base views of zigzag Cr doped BN-4 in the supercell where the axis in yellow denotes the z (tube) axis. B, N and Cr atoms are shown in rose, blue and purple, respectively.

The spin dependent DOS spectrum of zigzag Cr doped BN-4 is presented in Figure 4.13. Spin asymmetric variation is observed due to the unoccupied d orbitals of the transition metal Cr atom. Majority and minority E_g were obtained as 0.54 eV and 1.64 eV, respectively as displayed in Figure 4.13. When the BNNT was doped by Cr, the DOS spectrum was significantly modified (see Figure 4.11 and 4.13). The DOS in conduction band is close the zero, whereas certain peaks due to majority and minority electrons were observed at energies $E < -1.4$ eV. There was only a little minority DOS peak seen around the E_F . It implies that the Cr doped BNNT shows almost half metallic

property which is required in the field of spintronics. Perfect half metallic systems, for which majority or minority DOS must be zero in the vicinity of E_F , give 100% spin polarization.

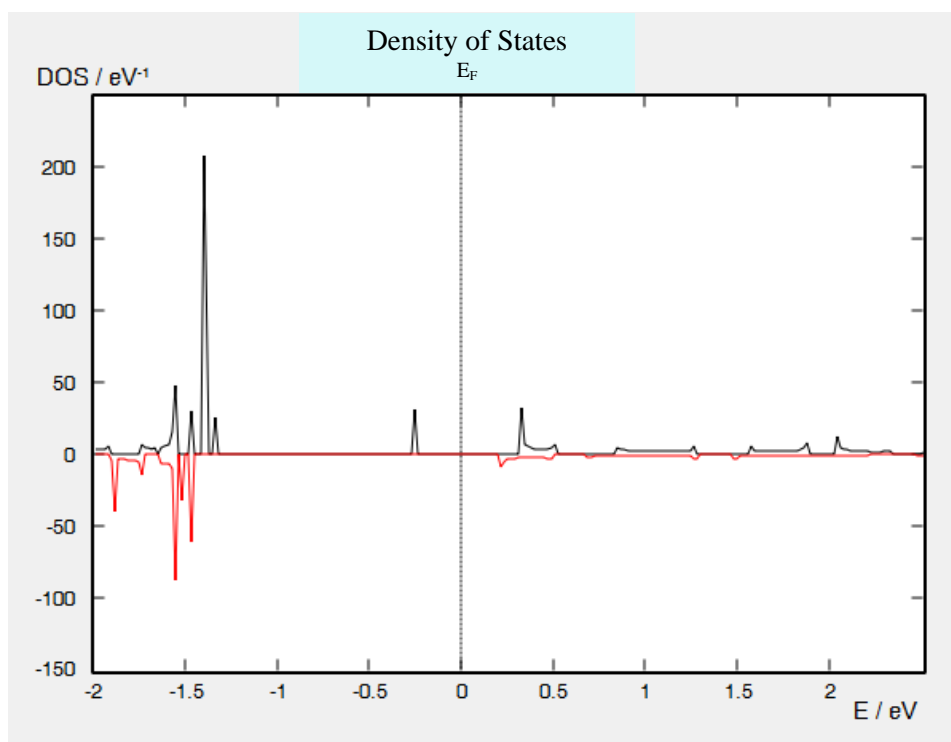


Figure 4.13 DOS spectrum of zigzag Cr doped BN-4 in the presence of spin. Black (positive) and red (negative) variations indicate the majority and minority DOS, respectively.

4.3.3 Ni Doped BN-4

Here, Cr was replaced by Ni atom and then Ni doped BN-4 was relaxed. The optimized structure is shown in Figure 4.14. In the optimized structure, the bond lengths between Ni atom and its nearest-neighbor N atoms were calculated to be 1.86 Å (the distance along the tube) and 1.81 Å. In the Ni doped BN-4 structure, the emerging average magnetic moment per atom was $0.021\mu_B$. Upon introducing a single Ni atom, we aimed at to see possible spin asymmetric variation in DOS and to observe if we expose the half metallicity of the Ni doped BN-4.

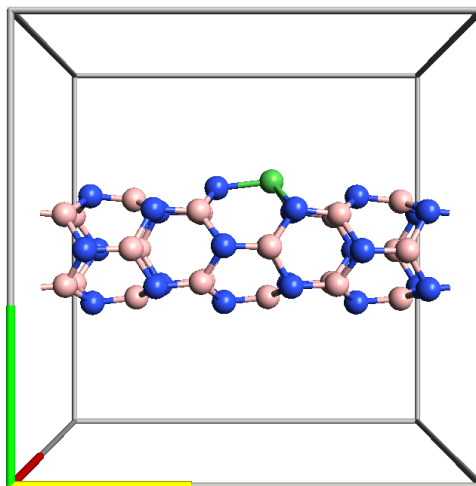


Figure 4.14 Side view of zigzag Ni doped BN-4 in the supercell where the axis in yellow denotes the z (tube) axis. B, N and Ni atoms are shown in rose, blue and green, respectively.

The spin dependent DOS spectrum for Ni doped BN-4 is displayed in Figure 4.15. When the system was doped by a single Ni atom, the majority and minority DOS were significantly modified. E_g was obtained as 0.01 eV and 1.04 eV for majority and minority electrons, respectively. We observed that the majority DOS is finite with abrupt peaks at energies close to E_F , however the minority DOS is zero around the E_F for a wide energy interval as shown in Figure 4.15. The spin asymmetry arising in this system was different than that in Co and Cr doped BN-4. Hence the associated spin polarization in the vicinity of the E_F was also changed. We found that for the Ni doped BN-4, a perfect half metallic property was almost revealed as minority DOS became zero at the E_F and majority E_g was close to zero. Hence this system in bulk or device form is promising for the possible spintronic applications in technology.

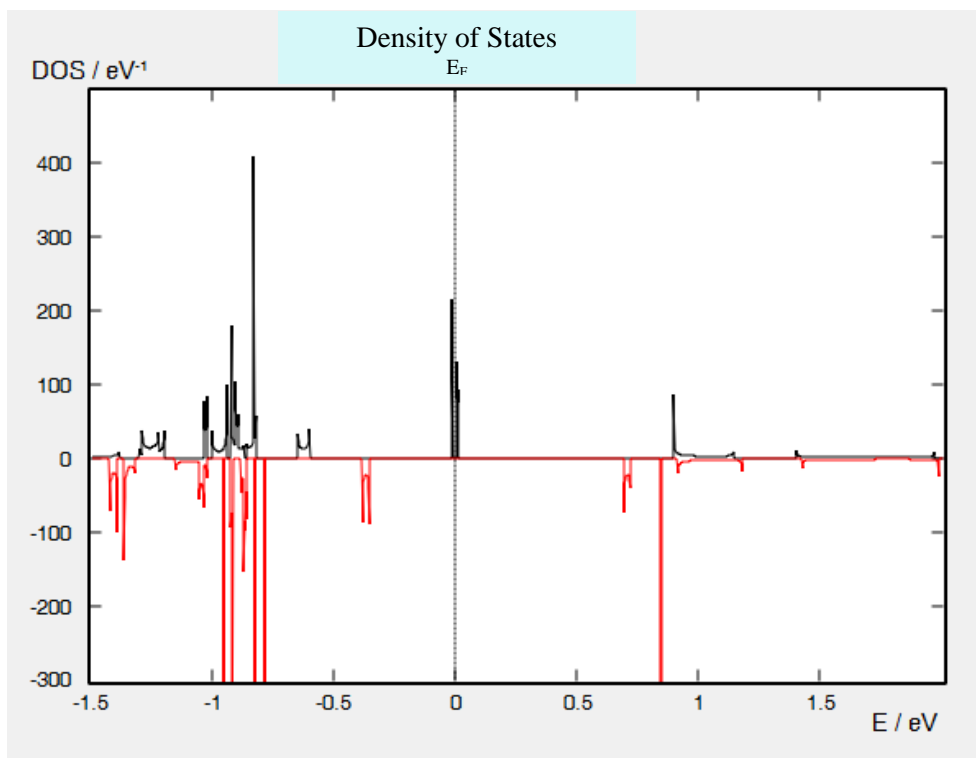


Figure 4.15 DOS spectrum of zigzag Ni doped BN-4 in the presence of spin. Black (positive) and red (negative) variations indicate the majority and minority DOS, respectively.

4.3.4 Au Doped BN-4

In addition to Co, Cr and Ni, we also examined Au doped BNNTs for the sake of comparison. Upon introducing a single Au atom, the system was relaxed. The optimized Au doped BN-4 system, where a single B atom has now been replaced by the Au atom, is shown in Figure 4.16. In relaxed system, the bond lengths between Au atom and its nearest-neighbor N atoms were 2.23 Å (the distance along the tube) and 2.07 Å. In the Au doped BN-4, the induced average magnetic moment per atom was found to be 0.042 μ_B .

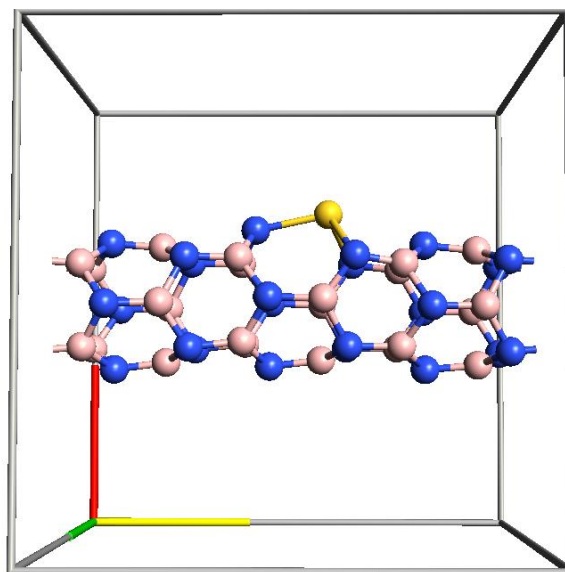


Figure 4.16 Side view of zigzag Au doped BN-4 in the supercell where the axis in yellow denotes the z (tube) axis. B, N and Au atoms are shown in rose, blue and yellow, respectively.

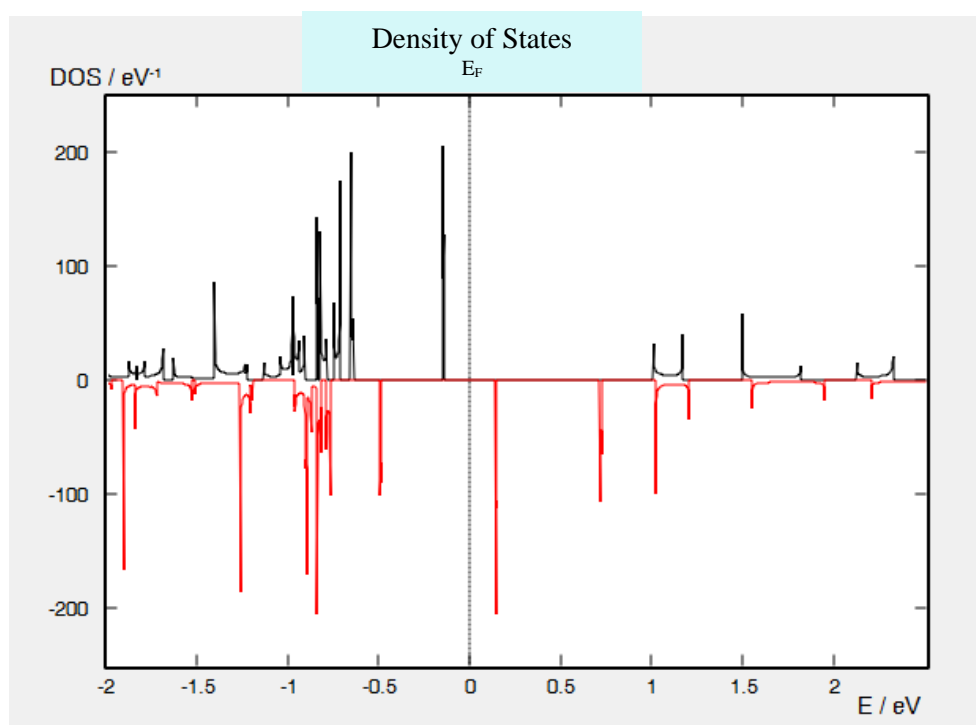


Figure 4.17 DOS spectrum of zigzag Au doped BN-4 in the presence of spin. Black (positive) and red (negative) variations indicate the majority and minority DOS, respectively.

The DOS spectrum for Au doped BN-4 in the presence of spin is presented in Figure 4.17. The majority and minority E_g were obtained as 1.15 eV and 0.62 eV, respectively. The majority DOS values were low in the conduction band but they were high in the valence band at particular negative energies, as shown in Figure 4.17. On the other hand, minority DOS exhibited certain huge peaks in both conduction and valence band. The number of peaks in the conduction band (at positive energies) is less than that in the valence band (at negative energies). In Au doped BN-4, as illustrated in Figure 4.17, we obtained a perfect semiconducting property which has spin dependent band structure.

Comparison of band gaps of zigzag pure BN-4, Co doped BN-4, Cr doped BN-4, Ni doped BN-4 and Au doped BN-4 is presented in Table 4.2. For the pure BN-4, E_g was 1.44 eV which is below the experimental values, due to the well known fact that DFT calculations underestimate the energy band gap (Eglitis R.I. et al.,2006). In order to improve this deficiency one may employ Hubbard correction (Hubbard J. 1963). The emerging spin dependent E_g was changed due to the type of the transition metal. The narrowest majority (minority) E_g was 0.01 eV (0.14 eV) obtained for Ni (Co) doped system and the widest one was 1.15 eV (1.64 eV) found for Au (Cr) doped BN-4. Among these systems, the most promising system to be applied in spintronics is the Ni doped BNNT since it almost exhibited a perfect spin polarization or half metallic property. But the other systems may also be employed in this field through playing the dopant concentration or its position, which may give rise to a high spin polarization at the E_F . From the DOS spectra of each doped system, we see that the spin unrestricted electronic structure behavior or electronic transport properties can be varied by means of transition metals. Thus introducing a particular dopant concentration at certain locations in the system one may obtain a desired spin dependent electronic feature in zigzag BNNTs. The spin dependent behavior is related to emerging magnetism, yielding a magnetic moment in the system. The associated average magnetic moment for each system is given above and also tabulated in Table 4.3.

Table 4.2 Comparison of band gaps of zigzag pure BN-4, Co doped BN-4, Cr doped BN-4, Ni doped BN-4 and Au doped BN-4.

System	Number of Atoms in the Supercell	Exchange Correlation Functional	Band Gap (eV)
Pure BN-4	16	GGA.PBE	1.44
Co doped BN-4	48	SGGA.PBE	0.73 (majority)
			0.14 (minority)
Cr doped BN-4	48	SGGA.PBE	0.54 (majority)
			1.64 (minority)
Ni doped BN-4	48	SGGA.PBE	0.01 (majority)
			1.04 (minority)
Au doped BN-4	48	SGGA.PBE	1.15 (majority)
			0.62 (minority)

Table 4.3 Average magnetic moment per atom, emerging in Co doped BN-4, Cr doped BN-4, Ni doped BN-4 and Au doped BN-4, for a specific dopant concentration.

System	Dopant Concentration	Average magnetic moment per atom (μ_B)
Co doped BN-4	2.1%	0.036
Cr doped BN-4	2.1%	0.063
Ni doped BN-4	2.1%	0.021
Au doped BN-4	2.1%	0.042

4.4 POSITION OF TRANSITION METAL ATOM

In addition to the type of the transition metal atom, we also examined the effect of location of dopants in zigzag BNNTs on the spin dependent electronic structure properties. For instance, we intended to observe the possible change in majority and minority energy band gap due to the position of the substitutionally added transition metal dopant in any BNNT structure. We utilized one of the aforementioned systems, where each dopant was placed in the middle of the BN-4, to see this effect. We employed Co doped BN-4 where Co atom was first located at the left side and then placed at the right side of the BN-4, as shown in Figure 4.18. The obtained spin dependent band gap values are tabulated in Table 4.4. Spin dependent E_g remained the same if the Co was located in the middle or at the left side of BN-4. However, when the Co atom was placed at the right side of BN-4, we observed a change in both majority and minority E_g as seen in Table 4.4. It implies the role of position of transition metal dopant in BNNTs on the electronic structure properties.

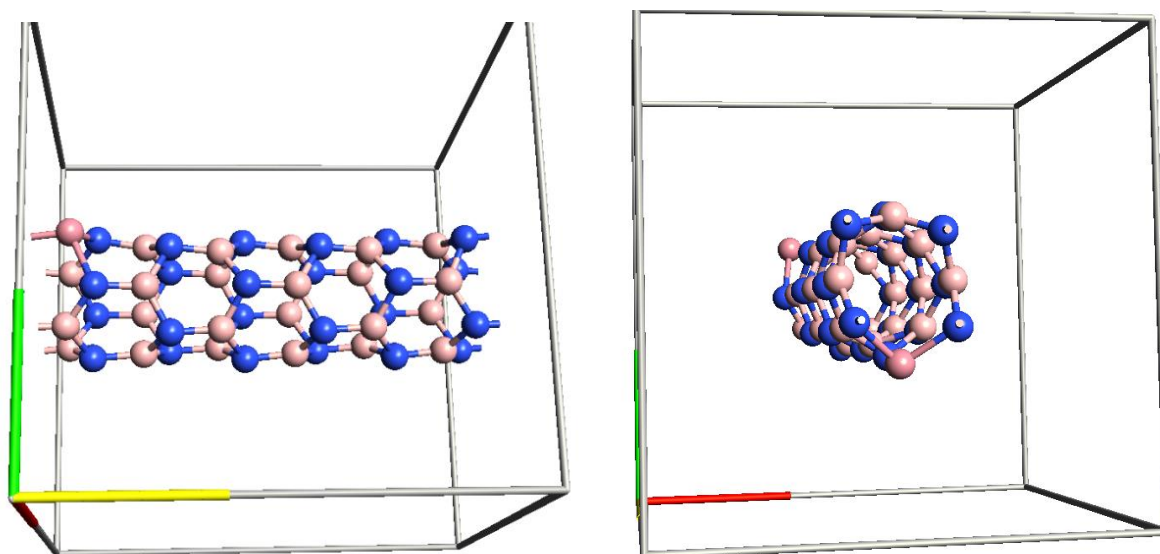


Figure 4.18 Zigzag Co doped system. Co is located at (a) left and (b) right side of BN-4 in the supercell. B, N and Co atoms are shown in rose, blue and dark pink, respectively.

Table 4.4 Spin dependent band gap of a zigzag Co doped BN-4 when Co atom is placed in the middle, at the left and right side of the BN-4.

Co doped BN-4	E_g (eV)	
	Majority	Minority
Co location: middle	0.73	0.14
Co location: left	0.73	0.14
Co location: right	0.19	0.13

CHAPTER 5

CONCLUSION

In this thesis, we considered both pure and transition metal atom doped BNNTs applying the DFT calculations. We performed the first principles DFT calculations through the software package ATK. The dopants were substitutionally introduced to the system where host B atoms were replaced by dopants. We mainly concentrated on electronic structure properties of BNNTs with various radii in the absence and presence of spin. These properties were revealed in terms of tube radius, dopant type and its position in the supercell. We only focused on *zigzag* BNNTs with chiral vectors $(n,m) = (4,0)$, $(6,0)$ and $(8,0)$. Increasing n implies enhancing the radius of the tube. The BNNTs constructed were periodic or infinite along the z (or tube) axis. The dopants were chosen as transition metal atoms as their unoccupied d orbitals can induce spin polarization or magnetism in a system. The spin polarization was absent in pure BNNTs, whereas in doped structures it was observed. Even a single substitutional dopant is able to result in a spin asymmetry, for instance, in the density of states spectrum or spin unrestricted electronic structure behavior. Because of the emerging magnetism in doped BNNTs, the magnetic properties were also investigated, employing the Mulliken population. In general we examined these structures with low concentration of dopants. Our results showed that the band gap of BNNTs and the electronic structure properties (in the absence and presence of spin) were determined by its chiral vector or radius. From the density of states spectra of pure and doped BNNTs we obtained that both the position and type of dopants have enormous effect on the spin resolved electronic structure and transport behavior. According to the findings in the present study, one can deduce that BNNTs can be utilized in novel technology. They can also be efficiently employed in the field of spintronics as fundamental structures if one achieves a perfect spin polarization at the Fermi energy. We revealed that it is possible to obtain an almost perfect spin polarization if the BNNTs are doped by Ni

atoms. It implies that one is able to get a half metallic doped BNNT to be applied in the field of spintronics. This work can be extended to include device structures which will be formed by a BNNT system attached to the metallic electrodes. In this way, one is able to investigate the electron transport, through the BNNT, and current-voltage characteristics.

REFERENCES

- Akdim B., Pachter R., Duan X. and Adams W.W., "*Comparative theoretical study of single-wall carbon and boron-nitride nanotubes*" Physical Review B, Vol.67, pp.147-148, 2003
- Aqel A., Kholoud M.M., El-Nour A. , Reda A.A. Ammar and Al-Warthan A., "*Carbon nanotubes, science and technology part (I) structure, synthesis and characterisation*" Arabian Journal of Chemistry, Vol.5, pp.1-23, 2012
- Baibich M. N., Broto J. M., Fert A., Nguyen Van Dau F. N., Petroff F., Etienne P., Creuzet G. Friederich A. and Chazelas J. "*Giant Magnetoresistance of (001)Fe/(001)Cr Magnetic Superlattices*". Physical Review Letters, Vol.61, pp. 2472-2475, 1988
- Bian L. and Zhao H., "*Elastic properties of a single-walled carbon nanotube under a thermal environment*" Composite Structures Vol.121, pp.337-343, 2014
- Blase X., Rubio A., Louie S.G. and Cohen M.L., "*Stability and Band Gap Constancy of Boron Nitride Nanotubes*" Europhysics Letters Vol.8, 1994
- Ceperley D.M. and Alder B.J. "*Ground State of the Electron Gas by a Stochastic Method*" Physics Review Letters, Vol.45, pp.566, 1980
- Cheewawuttipong W., Fuoka D., Tanoue S., Uematsu H. and Iemoto Y., "*Thermal and Mechanical Properties of Polypropylene/Boron Nitride Composites*" Energy Procedia, Vol.34, pp.808-817, 2013
- Chen X., Wu P., Rouseas M., Okawa D., Gartner Z., Zettl A. and Bertozzi C.R., "*Boron Nitride Nanotubes Are Noncytotoxic and Can Be Functionalized for Interaction with Proteins and Cells*" Journal of the American Chemical Society, Vol.131, pp.890-891, 2009
- Chen Y., Zou J., Campbell S.J. and Caer G.L. "*Boron nitride nanotubes: Pronounced resistance to oxidation*" Applied Physics Letters, Vol.84, pp.2430-2433, 2004
- Chopra N.G., Luyken R.J., Cherrey K., Crespi V.H., Cohen M.L., Louie S.G. and Zettl A., "*Boron Nitride Nanotubes*" Science, New Series, Vol. 269, pp. 966-967, 1995

- Cumings J. and Zettl A., "*Mass-production of boron nitride double-wall nanotubes and nanococoons*" Chemical Physics Letters, Vol.316, pp.211-216, 2000
- Datta S. and Das B. "*Electronic Analog of the Electro-Optic Modulator*" Applied Physics Letters, Vol.56, pp.665-667, 1990
- Dhariwal S., Lamba V.K. and Vijay R. "*Modeling Transport Properties of Single-Wall Carbon Nanotube Between Metal and Graphene Electrodes*" Journal of Nanoengineering and Nanosystems, Vol.228, 2013
- Dowling A.P., "*Development of Nanotechnologies*" Materials Today, Vol.7, pp.30-35, 2004
- Eglitis R.I., Shi H. and Borstel G. "*First Principles Calculations of the CaF₂ Surface Electronic and Band Structure*" World Scientific Publishing Company, Vol.13, pp.149-154, 2006
- Ekli E. and Şahin N., "*Science Teachers and Teacher Candidates' Basic Knowledge, Opinions and Risk Perceptions about Nanotechnology*" Procedia Social and Behavioral Sciences, Vol.2, pp.2667-2670, 2010
- Engel E., Keller S. and Dreizler R. M. "*Generalized Gradient Approximation for the Relativistic Exchange-Only Energy Functional*" Physical Review A, Vol.53, pp.1367-1374, 1996
- Esrafil M.D. and Behzadi H. "*A DFT study on carbon-doping at different sites of (8, 0) boron nitride nanotube*" Structural Chemistry, Vol. 24, Issue 2, pp.573-581, 2012
- Govindaraju N. and Singh R.N., "Synthesis and Properties of Boron Nitride Nanotubes" Nanotube Superfiber Materials, Vol.6, pp.243-265, 2013
- Griebel M. and Hamaekers J., "*Molecular dynamics simulations of boron-nitride nanotubes embedded in amorphous Si-B-N*" Computational Materials Science, Vol.39, pp.502-517, 2007
- Guptaa A.K. and Harshaa S.P., "*Analysis of mechanical properties of carbon nanotube reinforced polymer composites using continuum mechanics approach*" 3rd International Conference on Materials Processing and Characterisation, Vol.6, pp.18-25, 2014
- Hao S., Zhou G., Duan W., Wu J. and Gu B.L. "*Tremendous Spin-Splitting Effects in Open Boron Nitride Nanotubes: Application to Nanoscale Spintronic Devices*" American Chemical Society Vol.128, pp.8453-8458, 2006
- Harigaya K., "*Excitons in optical spectra of boron–nitride (BN) nanotubes*" Journal of Physics and Chemistry of Solids, Vol.71, pp.627-629, 2010
- Hohenberg P. and Kohn W. "*Inhomogeneous Electron Gas*" Physical Review B, Vol.136, pp.864-871, 1964

- Hubbard J. *"Electron Correlation in Narrow Energy Bands"* Proceedings of the Royal Society of London, Vol.276, pp.238-257, 1963
- Hussein A.K., *"Applications of Nanotechnology in Renewable Energies—A Comprehensive Overview and Understanding"* Renewable and Sustainable Energy Reviews, Vol.42, pp.460-476, 2014
- Jhia S.H., Roundya D.J., Louie S.G. and Cohen M.L., *"Formation and electronic properties of double-walled boron nitride nanotubes"* Solid State Communications Vol.134, pp.397-402, 2005
- Johnson M. and Silsbee R.H. *"Interfacial charge-spin coupling: Injection and detection of spin magnetization in metals"*. Physical Review Letters, Vol.55, pp.1790-1793, 1985
- Jones R.O and Gunnarsson O. *"The Density Functional Formalism, Its Applications and Prospects"* Rev. Mod. Phys., Vol.61, pp.689, 1989
- Kohn W. and Sham L.J. *"Self-Consistent Equations Including Exchange and Correlation Effects"* Physical Review Letters, Vol.140, pp.1133-1138, 1965
- Kostoglou N., Polychronopoulou K. and Rebholz C., *"Thermal and Chemical Stability of Hexagonal Boron Nitride (h-BN) Nanoplatelets"* Vacuum, Vol.112, pp.42-45, 2014
- Krishnamurthy G., Namitha R and Agarwal S., *"Synthesis of Carbon Nanotubes and Carbon Spheres and study of their hydrogen storage by Electrochemical Method"* Procedia Materials Science, Vol.5, pp.1056-1065, 2014
- Lahiri D., Rouzaud F., Richard T., Keshri A.K., Bakshi S.R., Kos L. and Agarwal A., *"Boron nitride nanotube reinforced polylactide–polycaprolactone copolymer composite: Mechanical properties and cytocompatibility with osteoblasts and macrophages in vitro"* Acta Biomaterialia Vol.6, pp.3524-3533, 2010
- Lijima S. *"Helical Microtubules of Graphit Carbon"* Nature, Vol.354, pp.56-58, 1991
- Mashreghi A., *"Thermal expansion/contraction of boron nitride nanotubes in axial, radial and circumferential directions"* Computational Materials Science, Vol.65, pp.356–364, 2012
- Mishima O., Tanaka J., Yamaoka S. and Fukunaga O., *"High-Temperature Cubic Boron Nitride P-N Junction Diode Made at High Pressure"* Science, Vol. 238, pp.181-183, 1987
- Mohammad A.W., Lau C.H., Zaharim A. and Omar M.Z. *"Elements of Nanotechnology Education in Engineering Curriculum Worldwide"* Procedia Social and Behavioral Sciences, Vol.60, pp.405-412, 2012

- Mulliken R.S. *"Electronic Population Analysis on Molecular Wave Function"* The Journal of Chemical Physics, Vol.23, pp.1833-1840, 1955
- Oku T., Koi N. and Suganuma K., *"Electronic and optical properties of boron nitride nanotubes"* Journal of Physics and Chemistry of Solids, Vol.69, pp.1228-1231, 2008
- Pati R., Senapati L., Ajayan P.M. and Nayak S.K. *"First principles calculations of spin-polarized electron transport in a molecular wire: Molecular spin valve"* Physical Review B, Vol.68, 2003
- Perdew J.P. and Zunger A., *"Self-interaction correction to density-functional approximations for many-electron systems"* Physics Review B, Vol.23, 1981
- Perdew J.P., Chevary J.A., Vosko S.H., Jackson K.A., Pederson M.R. and Singh D.J., *"Applications of the Generalized Gradient Approximation for Exchange and Correlation"* Physics Review B, Vol.46, pp.6671-6687, 1992
- Porter A.L. and Youtie J., *"Where does nanotechnology belong in the map of science?"* Nature Nanotechnology, Vol.4, pp.534-536, 2009
- Purohit R., Purohit K., Rana S., Rana R.S. and Patel V., *"Carbon Nanotubes and Their Growth Methods"* 3rd International Conference on Materials Processing and Characterisation, Vol.6, pp.716-728, 2014
- Radosavljević M., Appenzeller J., Derycke V., Martel R., Ph. Avouris, Loiseau A., Cochon J.L. and Pigache D., *"Electrical properties and transport in boron nitride nanotubes"* Applied Physics Letters, Vol.82, Issue 23, 2003
- Rimola A. and Sodupe M. *"Gas-Phase and Microsolvated Glycine Interacting with Boron Nitride Nanotubes"* Inorganics, Vol.2, pp.334-350, 2014
- Sarma S.D. *"Spintronics: A new class of device based on electron spin, rather than on charge, may yield the next generation of microelectronics"* American Scientist, Vol.89, pp.516-523, 2001
- Sasaki O. and Ohta H. *"Boron Nitride Ceramics"* Met. Technol., Vol.56, pp.13-17, 1986
- Sellers K., *"Nanotechnology and the Environment"* Nanotechnology and the Environment CRC Press, Taylor & Francis Group, Vol.13, pp.296-297, 2010
- Steinborn C., Herrmann M., Keitel U., Schönecker A., Räthel J., Rafaja D. and Eichler J., *"Correlation between Microstructure and Electrical Resistivity of Hexagonal Boron Nitride Ceramics"* Journal of the European Ceramic Society, Vol.33, pp.1225-1235, 2013
- Vel L., Demazeau G. and Etourneau J., *"Cubic boron nitride: synthesis, physicochemical properties and applications"* Material Science and Engineering, Vol.10, pp.149-164, 1991

- Wang J., Lee C.H., Bando Y., Golberg D. and Yap Y.K., "*Multiwalled Boron Nitride Nanotubes: Growth, Properties, and Applications*" Lecture Notes in Nanoscale Science and Technology, Vol.6, pp.23-42, 2009
- Wei X., Wang M.S, Bando Y. and Golberg D., "*Tensile Tests on Individual Multi-Walled Boron Nitride Nanotubes*" Advanced Materials, Vol.22, Issue 43, pp.4895-4899, 2010
- Wolf S.A., Awschalom D.D., Buhrman R.A., Daughton J.M., von Molnár S., Roukes M.L., Chtchelkanova A.Y., Treger D.M. "*Spintronics: a spin-based electronics vision for the future*" American Association for the Advancement of Science, Vol.294, pp.1488-1495, 2001
- Xie Y., Huo Y.P. and Zhang J.M. " First-principles study of CO and NO adsorption on transition metals doped (8,0) boron nitride nanotube" Applied Surface Science, Vol.258, pp.6391– 6397, 2012
- Yap Y.K, Wang J. and Lee C.H., "*Recent Advancements in Boron Nitride Nanotubes*" The Royal Society of Chemistry, Vol.2, pp.2028-2034, 2010
- Zhang Z., Guo W. and Dai Y., "*Stability and electronic properties of small boron nitride nanotubes*" Journal of Applied Physics, Vol.105, Issue 8, pp.11-12, 2009
- Zhang Z.W., Zheng W.T. and Jiang Q., "*Hydrogen adsorption on Ce/BNNT systems: A DFT study*" International Journal of Hydrogen Energy, Vol.37, pp.5090-5099, 2012
- Zheng M., Chen X., Park C., Fay C.C., Pugno N.M. and Ke C., "*Nanomechanical cutting of boron nitride nanotubes by atomic force microscopy*" Nanotechnology Vol.24, Number 50, 2013
- Zhi C., Bando Y., Tang C. and Golberg D., "*Boron Nitride Nanotubes*" Materials Science and Engineering, Japan, Vol.70, pp.92-111, 2010
- Zhi C., Bando Y., Tang C., Honda S., Sato K., Kuwahara H. and Golberg D. "*Characteristics of Boron Nitride Nanotube–Polyaniline Composites*" Angewandte Chemie International Edition, Vol. 44, pp.7929-7932, 2005